



# NAVAL POSTGRADUATE SCHOOL

MONTEREY, CALIFORNIA

## THESIS

**DEVELOPMENT OF A HIGH-PRECISION SENSOR FOR  
THE ATTITUDE DETERMINATION OF THE BIFOCAL  
SPACECRAFT SIMULATOR**

by

Brian D. Connolly

June 2004

Thesis Advisors:

Brij Agrawal  
Marcello Romano

**Approved for public release; distribution is unlimited**

**THIS PAGE INTENTIONALLY LEFT BLANK**

## REPORT DOCUMENTATION PAGE

Form Approved OMB No. 0704-0188

Public reporting burden for this collection of information is estimated to average 1 hour per response, including the time for reviewing instruction, searching existing data sources, gathering and maintaining the data needed, and completing and reviewing the collection of information. Send comments regarding this burden estimate or any other aspect of this collection of information, including suggestions for reducing this burden, to Washington headquarters Services, Directorate for Information Operations and Reports, 1215 Jefferson Davis Highway, Suite 1204, Arlington, VA 22202-4302, and to the Office of Management and Budget, Paperwork Reduction Project (0704-0188) Washington DC 20503.

1. AGENCY USE ONLY (Leave blank)	2. REPORT DATE June 2004	3. REPORT TYPE AND DATES COVERED Master's Thesis
4. TITLE AND SUBTITLE: Development of a High-Precision Sensor for the Attitude Determination of the Bifocal Spacecraft Simulator		5. FUNDING NUMBERS
6. AUTHOR(S) Brian Dempsey Connolly		8. PERFORMING ORGANIZATION REPORT NUMBER
7. PERFORMING ORGANIZATION NAME(S) AND ADDRESS(ES) Naval Postgraduate School Monterey, CA 93943-5000		
9. SPONSORING /MONITORING AGENCY NAME(S) AND ADDRESS(ES) N/A		10. SPONSORING/MONITORING AGENCY REPORT NUMBER
11. SUPPLEMENTARY NOTES The views expressed in this thesis are those of the author and do not reflect the official policy or position of the Department of Defense or the U.S. Government.		
12a. DISTRIBUTION / AVAILABILITY STATEMENT Approved for public release; distribution is unlimited		12b. DISTRIBUTION CODE
13. ABSTRACT (maximum 200 words)		
<p>The Bifocal Relay Spacecraft attitude control simulator is under development in the Spacecraft Research &amp; Design Center of the Naval Postgraduate School. The objective of this simulator is to provide on-the-ground simulation of the dynamics and control of spacecraft for high precision Acquisition, Tracking and Pointing applications associated with space based laser relay. The required initial attitude determination accuracy for the Bifocal Relay Mirror test-bed is 10 <math>\mu</math>-radians. Normally, in laboratories where very high initial attitude knowledge is required, actual (space qualified) star trackers are incorporated into the testbed design. This is not possible at NPS as the laboratory does not have a skylight to allow visual access to the stars, and the photosensitive nature of many of the experiments would make such an opening inconvenient. Since it is critical to the operation of the testbed to provide accurate attitude knowledge, a substitute system was required.</p> <p>The present thesis documents the development of a new attitude sensor capable of providing attitude information within the required 10 <math>\mu</math>-radians (within a field of view of the order of 1 deg). The concepts leading up to the final design, the testing and selection of the equipment used in the final configuration, and a detailed explanation of how the final system calibration was performed are discussed in detail.</p>		

14. SUBJECT TERMS Star Tracker, Testbed, Laser Alignment, Attitude Determination		15. NUMBER OF PAGES 119	
16. PRICE CODE			
17. SECURITY CLASSIFICATION OF REPORT Unclassified	18. SECURITY CLASSIFICATION OF THIS PAGE Unclassified	19. SECURITY CLASSIFICATION OF ABSTRACT Unclassified	20. LIMITATION OF ABSTRACT UL

**THIS PAGE INTENTIONALLY LEFT BLANK**

**Approved for public release; distribution is unlimited**

**DEVELOPMENT OF A HIGH-PRECISION SENSOR FOR THE ATTITUDE  
DETERMINATION OF THE BIFOCAL SPACECRAFT SIMULATOR**

Brian D. Connolly  
Lieutenant, United States Navy  
B.A. Clinical Psychology, University of Montana, 1993

Submitted in partial fulfillment of the  
requirements for the degree of

**MASTER OF SCIENCE IN ASTRONAUTICAL ENGINEERING**

from the

**NAVAL POSTGRADUATE SCHOOL**  
**June 2004**

Author: Brian D. Connolly

Approved by: Dr. Brij Agrawal  
Thesis Advisor

Dr. Marcello Romano  
Thesis Co-Advisor

Anthony J. Healey  
Chairman, Department of Mechanical and  
Astronautical Engineering

**THIS PAGE INTENTIONALLY LEFT BLANK**

## ABSTRACT

The Bifocal Relay Mirror spacecraft attitude control simulator is under development in the Spacecraft Research & Design Center of the Naval Postgraduate School. The objective of this testbed is to provide on-the-ground simulation of the dynamics and control of spacecraft for high precision Acquisition, Tracking and Pointing applications associated with space based laser relay. The required initial attitude determination accuracy for the Bifocal Relay Mirror test-bed is  $10 \mu\text{-radians}$ . Normally, in laboratories where very high initial attitude knowledge is required, actual (space qualified) star trackers are incorporated into the testbed design. This is not possible at NPS as the laboratory does not have a skylight to allow visual access to the stars, and the photosensitive nature of many of the experiments would make such an opening inconvenient. Since it is critical to the operation of the testbed to provide accurate attitude knowledge, a substitute system was required.

The present thesis documents the development of a new attitude sensor capable of providing attitude information within the required  $10\mu\text{-radians}$  (within a field of view of the order of 1 deg). The concepts leading up to the final design, the testing and selection of the equipment used in the final configuration, and a detailed explanation of how the final system calibration was performed are discussed in detail.

**THIS PAGE INTENTIONALLY LEFT BLANK**

## TABLE OF CONTENTS

I.	INTRODUCTION.....	1
II.	ATTITUDE SENSOR .....	3
	A.    METHOD 1 – DIGITAL VIDEO CAMERA.....	3
	B.    METHOD 2 – LASER/PSD .....	3
	1.    Basic Geometry/Equipment Requirements .....	4
III.	INITIAL TESTING .....	7
	A.    PHASE I – TESTING LASER PERFORMANCE .....	7
	1.    Determining Laser Behavior .....	8
	a. <i>HeNe Results</i> .....	9
	b. <i>Polarized HeNe Results</i> .....	10
	c. <i>Diode Results</i> .....	11
	d. <i>Overall Comparison</i> .....	11
	2.    Performance at Steady State .....	12
	3.    Selecting a Laser .....	14
	B.    PHASE II – IMPROVING LASER PERFORMANCE.....	15
	C.    PHASE III – TESTING PSM PERFORMANCE.....	16
	1.    Sensor Fatigue.....	16
	2.    Sensor Sensitivity.....	17
	D.    PHASE IV – TESTING TOTAL SYSTEM PERFORMANCE.....	19
IV.	SENSOR LAYOUT .....	23
	A.    COMPONENT QUANTITIES .....	23
	B.    CHOOSING A LAYOUT.....	23
	C.    PLACEMENT OF THE PSMS .....	25
	1.    PSMs on Wall .....	25
	2.    Lasers on Wall .....	26
	3.    PSM/Laser Arrangement .....	27
	4.    Testbed Movement .....	28
V.	SENSOR KINEMATICS EQUATIONS .....	31
	A.    RELATING BEAM POSITION TO ROTATION .....	31
	B.    RELATING BEAM POSITION TO TIP/TILT .....	35
VI.	TESTBED/SENSOR SETUP .....	41
	A.    EQUIPMENT USED .....	41
	B.    STEP ONE – CALIBRATE THE MP5 .....	41
	C.    STEP TWO – POSITION TABLE.....	42
	D.    STEP THREE – REMOVE UPPER OPTICAL EQUIPMENT DECK ..	42
	E.    STEP FOUR – FIND THE TABLE CENTER .....	42
	F.    STEP FIVE – INERTIAL REFERENCE SYSTEM .....	43
	1.    Tape Measure Estimation.....	43
	2.    MP5 Correction and Verification .....	44

G. STEP SIX – ALIGN THE TESTBED TO THE INERTIAL REFERENCE FRAME.....	45
H. STEP SEVEN – INSTALL POSITION SENSING MODULES .....	47
I. STEP EIGHT – INSTALL THE DIODE LASERS .....	47
1. FOCUS .....	47
2. Align with Respect to Inertial.....	48
J. STEP NINE – INSTALL THE WALL MIRRORS .....	49
K. STEP TEN – INSTALL THE BEAM SPLITTERS.....	50
L. STEP ELEVEN – CALIBRATE THE PSMS.....	51
 VII. SENSOR CALIBRATION .....	53
A. ERROR BUDGET .....	55
 VIII. CONCLUSIONS.....	57
A. SUMMARY .....	57
1. Resolution .....	57
2. Precision.....	57
3. Accuracy .....	58
4. Limitations.....	58
a. <i>System Reset</i> .....	58
b. <i>Field of View (FOV)</i> .....	58
B. RECOMMENDATIONS .....	59
1. Include a Rough Sensor.....	59
2. Add a Second PSM to Each Sensor .....	59
3. Move Table Closer to Increase FOV .....	60
4. Use a Wavelength Discriminating Filter .....	60
5. Perform Testbed Alignment Kalman Filter (AKF) .....	60
 APPENDIX A – PSM DATASHEETS .....	61
APPENDIX B – OT301 AMPLIFIER DATASHEETS.....	65
APPENDIX C – HENE LASER DATASHEETS.....	69
APPENDIX D – POLARIZED HENE LASER DATASHEET .....	71
APPENDIX E – DIODE LASER DATASHEETS.....	73
APPENDIX F – AEROTECH NANO-POSITIONER DATASHEETS .....	75
APPENDIX G – LASERMARK® MP5 FIVE-BEAM LASER .....	81
APPENDIX H – MAGNETIC POLYCAST® PROTRACTOR.....	83
APPENDIX I – KINEMATIC MIRROR MOUNTS.....	85
APPENDIX J – KINEMATIC BEAM SPLITTER MOUNTS .....	87
APPENDIX K – CALIBRATION DATA .....	89
APPENDIX L –MATLAB CODE .....	95
LIST OF REFERENCES.....	101
INITIAL DISTRIBUTION LIST .....	103

## LIST OF FIGURES

Figure 1.	Artist rendition of the NPS Next Generation Testbed .....	1
Figure 2.	Laser test setup .....	7
Figure 3.	HeNe laser performance – $\frac{1}{2}$ Hz sampling for 8 hours.....	9
Figure 4.	Polarized HeNe laser performance – $\frac{1}{2}$ Hz sampling for 8 hours.....	10
Figure 5.	Diode laser performance – $\frac{1}{2}$ Hz sampling for 8 hours.....	11
Figure 6.	Reaching steady state operation .....	11
Figure 7.	HeNe Laser SS Performance (2000Hz for 60 Sec) .....	13
Figure 8.	SS performance comparison (left to right: HeNe, Diode, Polarized).....	14
Figure 9.	Improving Laser performance – running average .....	15
Figure 10.	Sensor fatigue test.....	17
Figure 11.	System performance test set-up.....	19
Figure 12.	Aerotech, Inc. tip/tilt and rotary position mounts .....	19
Figure 13.	Testing tip-down/tip-up sensitivity .....	20
Figure 14.	Artist rendition of the NPS Next Generation Testbed .....	24
Figure 15.	Initial Attitude Sensor configuration .....	25
Figure 16.	Design consideration one – PSMs on wall .....	26
Figure 17.	Design configuration two – Lasers on wall .....	26
Figure 18.	PSM layout considerations .....	27
Figure 19.	Finalized Sensor design .....	29
Figure 20.	Sensor layout – Top view .....	31
Figure 21.	Sensor layout – Side view .....	32
Figure 22.	Testbed rotation and sensor movement .....	32
Figure 23.	Rotation effect on PSD X-axis .....	33
Figure 24.	Star tracker model kinematic derivation points (rotation).....	33
Figure 25.	$\Delta X$ vs. $\gamma$ for small angles .....	35
Figure 26.	Star tracker modeler during testbed tilt.....	36
Figure 27.	Star tracker model kinematics derivation points(tilt/tip).....	37
Figure 28.	$\Delta Y$ vs. $\alpha$ for small angles.....	39
Figure 29.	Finding table center .....	43
Figure 30.	Inertial point estimation.....	44
Figure 31.	Aligning the table to the inertial axis .....	46
Figure 32.	Path length .....	48
Figure 33.	Gun-site view of diode laser alignment.....	48
Figure 34.	Semi-transparent 90° square.....	49
Figure 35.	Optical train cover.....	51
Figure 36.	Post calibration sensor readings (mm vs. # of samples for 10 seconds ).....	52
Figure 37.	The Nikon NE-20S Digital Theodolite .....	54
Figure 38.	Laser Wander differencing using opposing PSMs .....	59

**THIS PAGE INTENTIONALLY LEFT BLANK**

## LIST OF TABLES

Table 1.	PSD sensor readings.....	18
Table 2.	Developing the rotational kinematics .....	34
Table 3.	Developing the tip/tilt kinematics .....	38

**THIS PAGE INTENTIONALLY LEFT BLANK**

## ACKNOWLEDGMENTS

The author would like to thank several people for their contributions and assistance. Drs. Brij Agrawal and Marcello Romano at the Naval Postgraduate School gave considerable guidance, encouragement, and assistance in the development of the project. Dr. Nelson Pedreiro at Lockheed Martin assisted at several key points and ensured that the resources of LM were available whenever they were needed. Dr. Mark Pittelkau at Johns Hopkins University was kind enough to lend support in the sections relating to the Alignment Kalman Filter. All of the members of the Naval Postgraduate School Spacecraft Research and Design Center have my utmost respect and gratitude for their help in this endeavor.

**THIS PAGE INTENTIONALLY LEFT BLANK**

## I. INTRODUCTION

The Optical Relay Spacecraft Laboratory is a joint venture between the Naval Postgraduate School and the Air Force Research Laboratory. The project involves a multitude of Master's students, Doctoral students and post-Docs working alongside Distinguished Professors and leading industry experts to solve the complex problems of Acquisition, Tracking and Pointing (ATP) technologies for the Bifocal Relay Mirror spacecraft (BRMS). The BRMS consists of two optically coupled telescopes used to re-direct the laser light from a ground-based, aircraft-based or spacecraft-based laser to distant points on the earth, or to another spacecraft. The restrictions on pointing accuracy and jitter control for the optical payload are very tight.

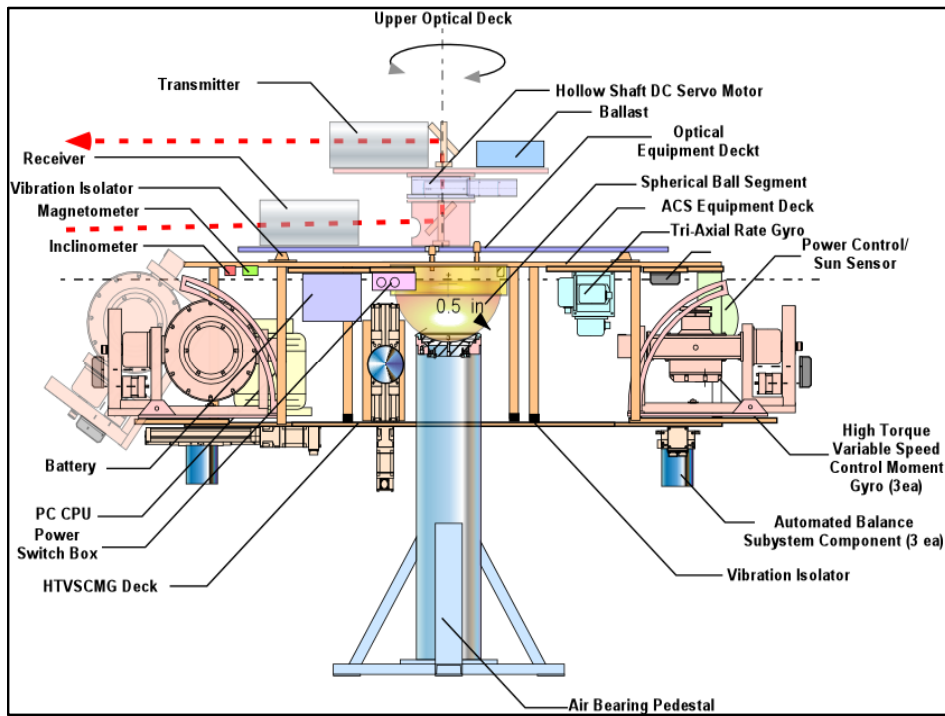


Figure 1. Artist rendition of the NPS Next Generation Testbed

To develop and demonstrate ATP technologies for the Bifocal Relay Mirror Spacecraft a new testbed is under development in the Naval Postgraduate School (NPS) laboratory (see Figure 1). This testbed consists of four main decks

mounted on a hemispherical air-bearing. The upper optical deck is capable of independent rotation, enabling independent tracking for the receive and transmit telescopes. This platform springs from the work of numerous students and instructors and will provide research opportunities for many more [1-7]. The testbed is being developed (where possible) with space-qualified components; however because it is a testbed, not every subsystem can be replicated using the exact hardware found on orbit: the attitude sensor is example.

In many laboratories where very high initial attitude knowledge is required, actual (space qualified) star trackers are incorporated into the testbed design. This is not feasible at NPS however; as the laboratory does not have a skylight to allow visual access to the stars, and the photosensitive nature of many of the experiments would make such an opening inconvenient. Additionally, the expense associated with a space qualified star-tracker was prohibitive. Since it is critical to the operation of the testbed to provide accurate attitude knowledge (accurate to within 10  $\mu$ -radians); a substitute system must be implemented. The objective of this research work was to develop an affordable model for a star tracker capable of providing very fine initial attitude knowledge.

The thesis will consist of the following areas:

1. Sensor Design
2. Determination of Component Performance
  - a. Position Sensing Device Performance
  - b. Laser Performance
  - c. Testing of System Performance
3. Sensor Configuration
4. Sensor Kinematic Equation Development
5. Sensor Integration and Testing
6. Sensor Calibration

## II. ATTITUDE SENSOR

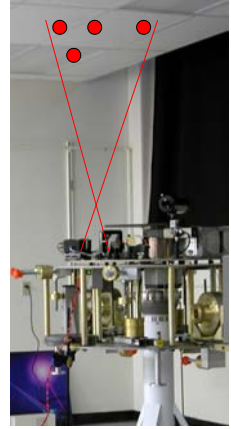
Two types of attitude sensors were evaluated: a digital video camera and a laser/sensor combination.

### A. METHOD 1 – DIGITAL VIDEO CAMERA

Initially; consideration was given to constructing a model star tracker using a digital video camera to mimic the lens structure, and a charge coupled device (CCD) sensor. In principle, by placing LEDs on the ceiling and using the camera to distinguish position relative to a known constellation, attitude could be established along all 3 axes.

Analysis of the situational geometry [taking into account the requirement for  $10 \mu\text{radian}$  pointing knowledge ( $\Theta$ ), and allowing for a 2 meter distance to target] gives:

$$\sin(\theta) = \frac{x}{2m} \Rightarrow \sin(10^{-5}) * 2m = x = 2 * 10^{-5} m$$



where  $x$  is the separation distance (that must be resolved by the system camera).

Resolution is a function of distance, lens size and pixel size. Allowing for a high-end commercial pitch (where pixel size  $\approx 10$  micron) the lens focal length<sup>1</sup>:

$$f\ell = \text{pixelsize} * \text{dist} / \text{separation} = 10^{-5} m * 2m / 2 * 10^{-5} m = 1m$$

The cost and weight of a one meter optic makes this method untenable.

### B. METHOD 2 – LASER/PSD

In many other applications within the Spacecraft Research and Design Center(SRDC) position sensing detectors (PSDs) have been used to determine laser beam position with extreme accuracy. [PSDs consist of a supporting

---

<sup>1</sup> *Remote Sensing from Air and Space*, p. 86.

substrate under a photovoltaic material which produces a voltage proportional to distance from center.] By using lasers sources as “stars” placed in known (fixed) locations, and mounting the PSDs on the testbed to sense where the “starlight” impacted the testbed, vectors to a known (inertial) reference system can be determined. The purpose of the following work is to determine whether it is possible to achieve initial position knowledge accurate to within  $10\mu\text{-radians}$  using this equipment.

## 1. Basic Geometry/Equipment Requirements

From above [taking into account the requirement for  $10\mu\text{rad}$  pointing knowledge ( $\Theta$ ), and allowing for a 2 meter distance to target]:

$$\sin(\theta) = \frac{x}{2m} \Rightarrow \sin(10^{-5}) * 2m = x = 2 * 10^{-5} m$$

where x is the separation distance (the absolute minimum discrimination the PSD must be capable of).

In order to conform to current lab equipment, position sensing modules (PSMs) produced by ON-TRAK Photonics, Inc. were evaluated for criterion compatibility (See Appendix A – PSM DATASHEETS). These devices consist of a silicone photovoltaic PSD encased in a protective aluminum case. The combination of PSD, the plug-and-play connection and the protective aluminum case is called a Position Sensing Module (PSM). The PSM is designed to work (plug-and-play) with ON-TRAK’s amplification system to provide an analog voltage output directionally proportional to distance from sensor center-point. To increase the range of motion sensitivity (field of view) for the testbed PSMs with 20mmx20mm sensors were chosen. These duolateral (two axes) silicon sensors provide position information in both x and y direction with respect to the sensor center. The ON-TRAK OT301 amplifier was also selected (for conformity with current lab equipment and familiarity of use) See

APPENDIX B – OT301 AMPLIFIER DATASHEETS for details. For analog to digital conversion and digital processing, the Keithley Instruments, Inc KPCI-

1802HC PCI bus data acquisition board was selected. This 12 bit card allows  $2^{12}$  or 4,096 quantization levels<sup>2</sup>. For a 20mm sensor this means the PSM should be capable of discriminating  $4.883 \times 10^{-6}$  meters, more than sensitive enough given the geometry requirement above. In order to prove the capabilities of the PSMs, and to determine what kind of laser would best suit the needs of the system, a series of testing was implemented.

---

<sup>2</sup> Keithley User's Manual, p. A-7.

**THIS PAGE INTENTIONALLY LEFT BLANK**

### III. INITIAL TESTING

Since the initial position is to be determined using laser impingement on a fine mesh PSD, it is critical to determine the performance capabilities of both the lasers and the PSDs.

#### A. PHASE I – TESTING LASER PERFORMANCE

Previous experiences from within the SRDC indicate that different types of lasers (HeNe, diode, argon, etc) have different performance capabilities. Further, it has been demonstrated that the performances of these lasers can vary over time (i.e. over several hours of continuous use, some laser's performance seems to improve, and some to degrade – allowing the beam to wander or bloom). In order to baseline the laser performance, and determine the optimal (most suitable for this application) style and time frame for each laser, the experimental set-up shown in Figure 2. was designed and implemented.

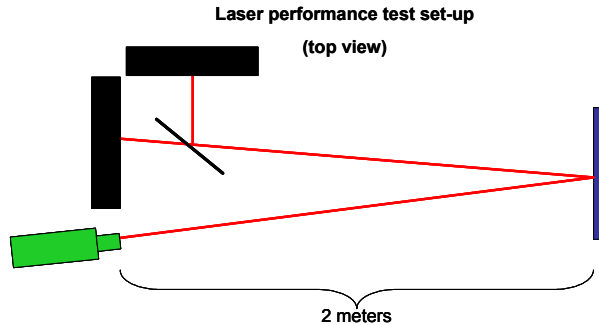


Figure 2. Laser test setup

The setup consists of a single mirror reflecting to a beam splitter then to two PSMs. Two PSMs were used to remove the possibility of attributing a sensor flaw to laser performance. The use of a mirror to return the beam to its approximate starting position minimizes the effects of air distortion (refraction) on the beam; thereby increasing the sensitivity of the measurements. The entire experimental setup was mounted on a Newport air table to minimize environmental vibration interference.

The following three types of laser sources were chosen for consideration in the final design:

- a Helium-Neon (HeNe) laser
  - model: Novette<sup>TM</sup> 1507-0 series self contained HeNe laser
  - manufactured by: JDS Uniphase Corporation
- a polarized HeNe laser
  - model: 31-2025-000 632.8 nm Red Cylindrical HeNe Laser
  - manufactured by: Coherent Technologies Inc.
- a small diode laser
  - model: UL12-1G-635 UL-series enclosed module diode laser
  - manufactured by: World Star Technology Inc.

See Appendices C-E for details/datasheets.

## **1. Determining Laser Behavior**

The lasers were mounted one-by-one into the setup as depicted above, and then put through a series of tests in order to determine what the best (defined as most stable) performance capability was, and how long it took for the laser to reach a stable condition. The tests varied in length (from a few seconds up to 12 hours) and in sampling frequency [from  $\frac{1}{2}$  Hz up to 4999 Hz (the limit of the analog to digital converter capability)]. After reviewing the results from the initial runs, it was decided that  $\frac{1}{2}$  Hz sampling over several hours would provide adequate information to determine steady state operation.

### a. HeNe Results

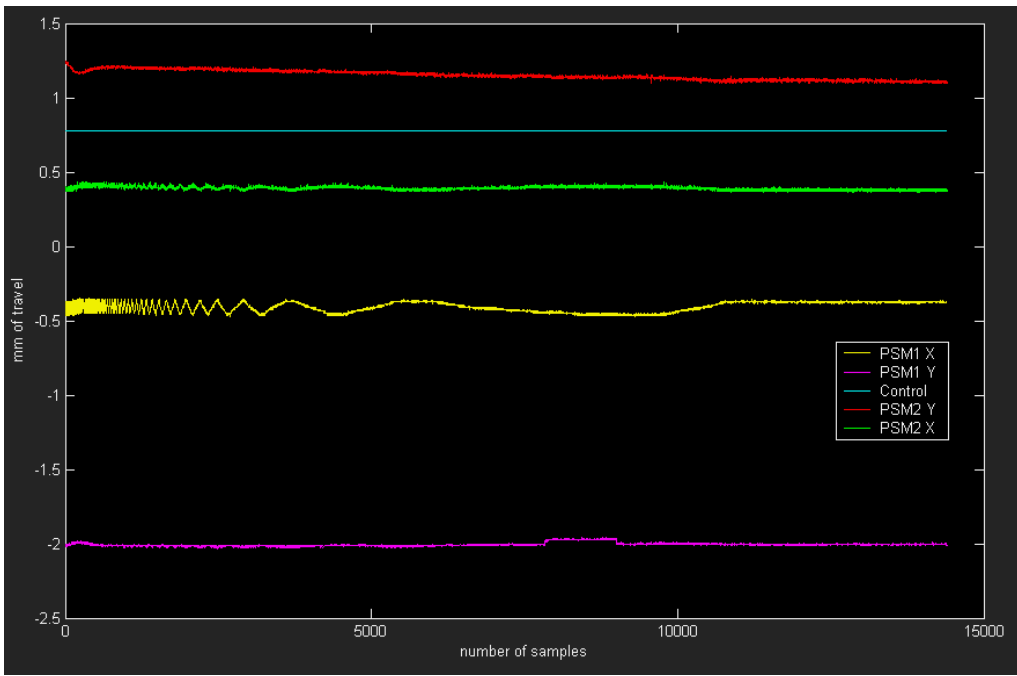


Figure 3. HeNe laser performance –  $\frac{1}{2}$  Hz sampling for 8 hours

Graphic explanation of Figure 3. :

- PSM1 X (yellow) – the horizontal component of PSM1
- PSM1Y (purple) – the vertical component of PSM1
- Control (blue) – a constant DC input
- PSM2 Y (red) – the vertical component of PSM2
- PSM2 X (green) – the horizontal component of PSM2

A reference constant voltage signal was used to check the level of system noise. This input (a stable DC voltage sent directly into the analog to digital signal converter) was also plotted on the graph. Note that while some noise is present in the system, it remains smaller than the data acquisition quantization (which is  $1.165 \times 10^{-12}$  radians or 1.2 picoradians). The result (depicted in Figure 3. ) is a continuous straight line. Note also that, due to the alignment of the sensors on the Newport table, PSM1 Y and PSM2 Y were reversed. In other words, since PSM 2 is mounted upside down, whenever Y1 goes up, Y2 goes down.

As shown in Figure 3. , the HeNe laser took approximately 30 min to stabilize in the Y direction, and an average of 6.3 hours to stabilize in the X

direction. The apparent sinusoidal motion in the X direction has been determined to be due to the age of the laser. Indeed, the resonating chamber in the Novette™ is made of glass; which is slightly permeable to Helium. Over time, some of the stabilizing Helium has dissipated from the chamber requiring a much longer lead time to reach steady state.

**b. Polarized HeNe Results**

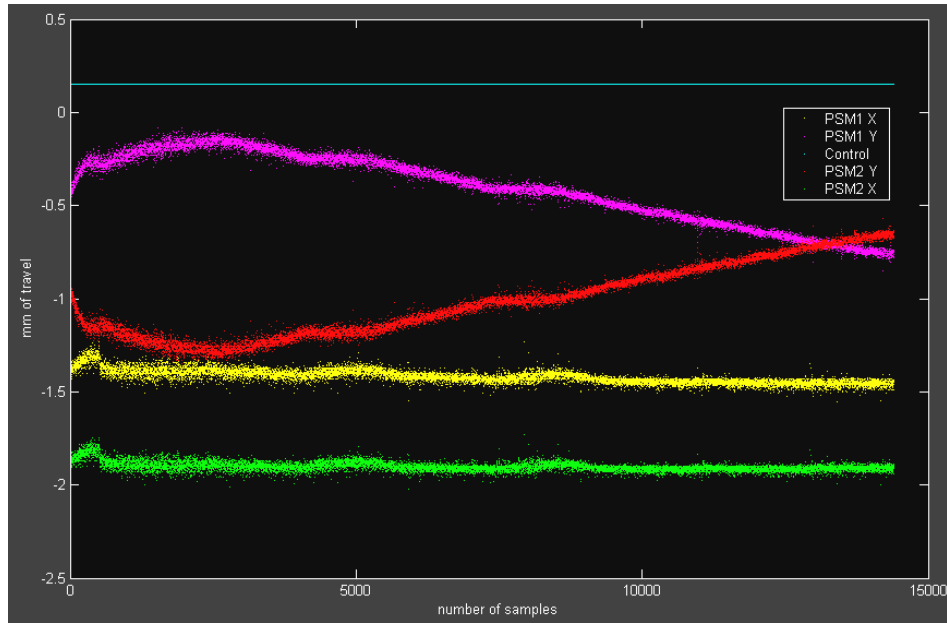


Figure 4. Polarized HeNe laser performance –  $\frac{1}{2}$  Hz sampling for 8 hours

According to the manufacturer's datasheet (reported in APPENDIX D) the stability of this laser should be smaller than  $<0.03$  mrad of drift after a 15 min warm-up. According to our tests, the unit failed to meet this criterion. Following a 20 min warm-up, the laser fluctuated over a range  $>0.08$  mrad (more than twice the advertised amount). Moreover, as shown in Figure 4. the laser failed to reach steady a state in 8 hours. It was only after the 10 hour point that the laser reached a “steady” ( $<0.03$  mrad drift) state (See the section on steady state behavior below). Note also that the plotted positions of the polarized laser create much thicker “lines” than that of the HeNe above. This is a result of the polarized unit having a higher bloom rate than the other lasers.

### c. Diode Results

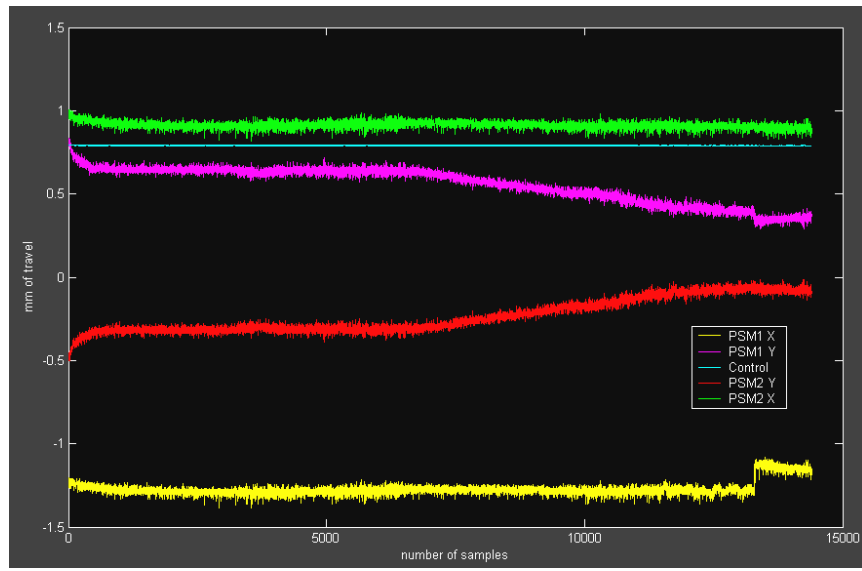


Figure 5. Diode laser performance –  $\frac{1}{2}$  Hz sampling for 8 hours

This laser behaved very much as expected: after an initial warm-up period (of approx 22 min) the laser reaches a stable, steady state operation that lasts for approx 4 hours. After 4 hours of continuous operation the dielectric material begins to overheat, causing some instability in both the x and y axes (beam wander). This can be overcome by giving the laser a brief (30 min) cool-down, or by actively cooling the laser.

### d. Overall Comparison

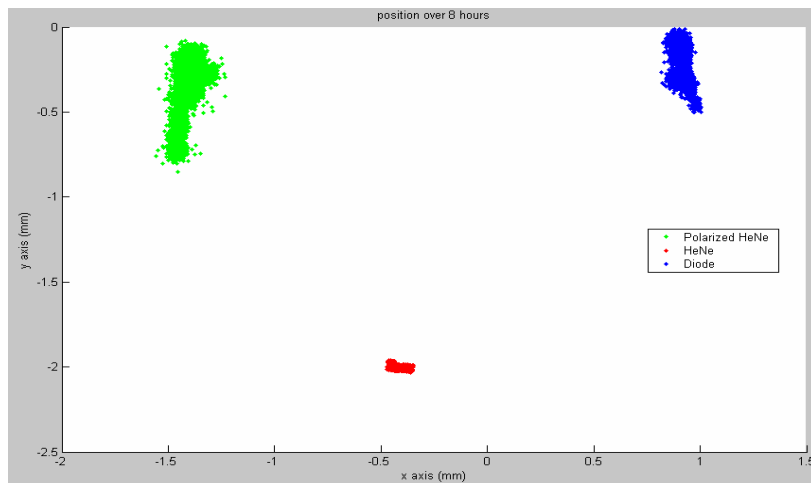


Figure 6. Reaching steady state operation

An initial glimpse into laser behavior showed that of the 3 units tested (see Figure 6. ), the HeNe showed the least amount of drift/bloom while getting to steady state. This was not, however the critical criterion. The laser which demonstrated the most reliable, stable characteristics while in steady state operation is what was needed.

## 2. Performance at Steady State

Steady state performance was measured in the same setup described in Figure 2. The exception was that lasers were brought to their optimum steady state operation times (6.3 hour warm-up for HeNe, 10 hours for Polarized, and 22 min for the diode) and tested at 2000Hz for 60 seconds. The results were graphed differently than above (see Figure 7. ).

- In the upper left is the familiar graph of Y and X vs. # of samples.
- In the upper right is a graph of Y vs. X (in mm). This graph; however is insufficient to determine stability. Note that 2000Hz sampling for 60 seconds will result in 120,000 samples. In the upper right graph the (X,Y) points may be repeated many times, but show no effective “weight” to aid in determining average laser position. Therefore:
- The lower right graph includes a weighting factor. The points that are singular appear as dark blue – the most repeated points in red.

- The lower left chart is a 3-D histogram created to demonstrate laser stability. The more frequently a point was hit, the “taller” it becomes on the graph. (Axes are mm x mm x number of occurrences)

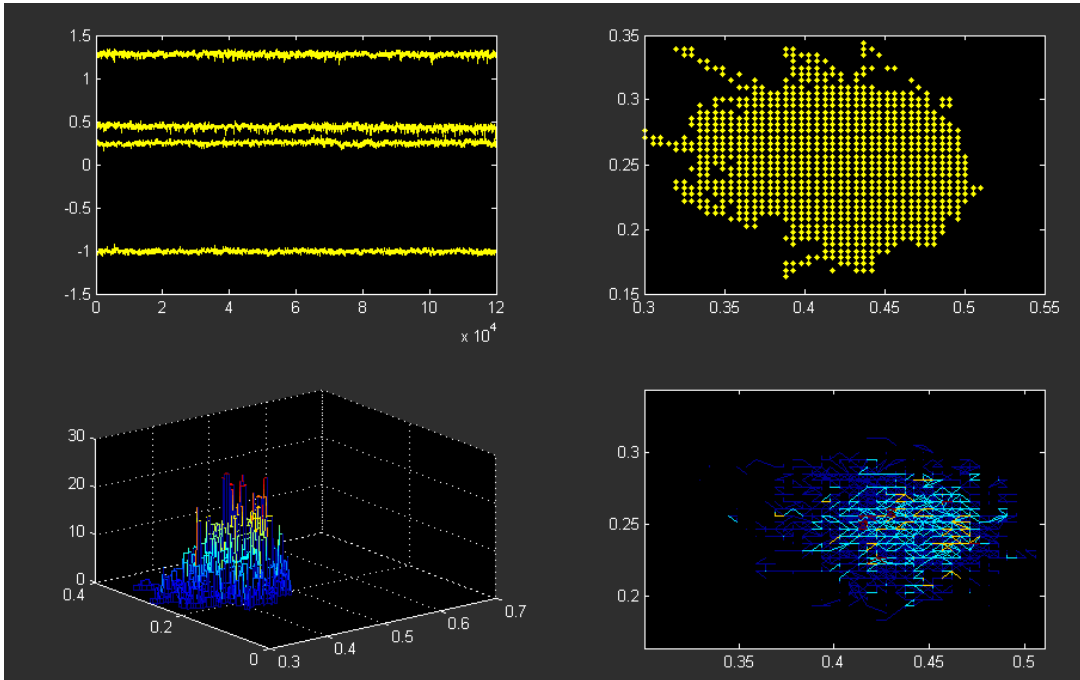


Figure 7. HeNe Laser SS Performance (2000Hz for 60 Sec)

Since the purpose of this phase of testing was to compare the performance of the different lasers, data from each laser was graphed on the same plane in order to provide a comparative analysis tool (see Figure 8. mm x mm x number of occurrences).

When graphed together:

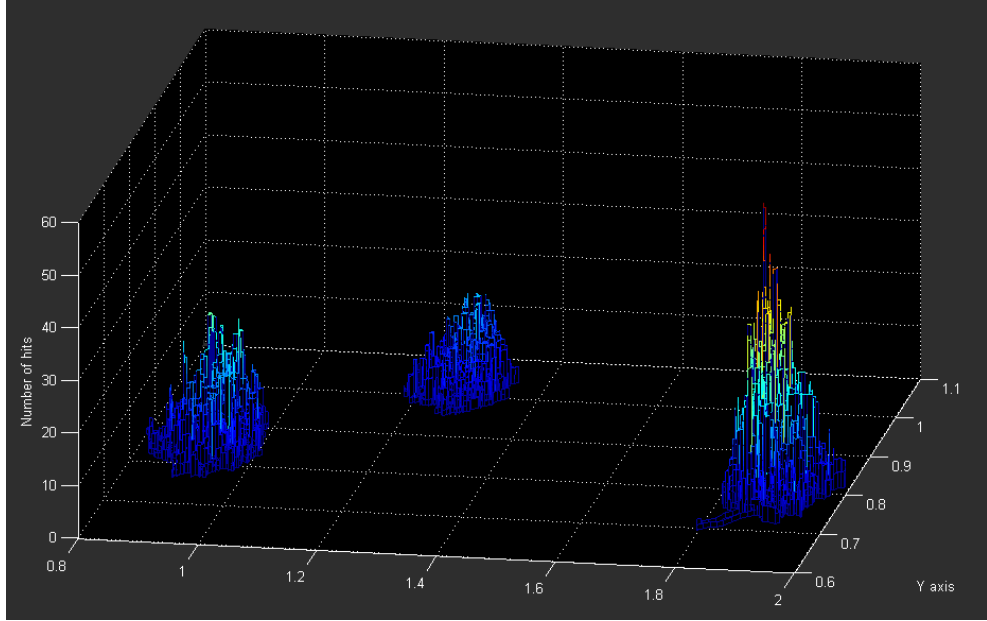


Figure 8. SS performance comparison (left to right: HeNe, Diode, Polarized)

While the performances of the three lasers while in steady state appear nearly identical, some distinct trends exist. Repeated experiments produce very similar results: mainly that the polarized laser had the greatest “center of mass” (highest histogram) but also the greatest base size. The diode laser always had the lowest, most consistent height and the smallest base area. Analysis of these trends indicated that the polarized unit tended to wander less frequently than the other lasers; however when wander does occur it was more severe. The diode laser histograms indicate that it tended to be the most consistent (predictable) performer.

### 3. Selecting a Laser

Since the final design will require measuring the angular position of the laser line, the total amount of beam wander must be minimized. The polarized laser may wander less frequently (though only marginally so) however it demonstrated the greatest amount of total travel, and thus exhibited the greatest angular instability. The diode laser consistently demonstrated the capacity to

constrain its wander to a fairly small area (smallest angular movement of the three lasers) and thus was considered to be the most consistent, well behaved steady state performance laser.

The diode laser had other advantages as well: it was very small, had lower power requirements, it was very inexpensive (a fraction of the cost of either HeNe design), and reached steady state operation in minutes. For these reasons the diode laser was selected for the final design.

## B. PHASE II – IMPROVING LASER PERFORMANCE

Even though the diode laser was chosen as the most stable laser, the question of “Is it good enough?” remained. Since the testbed attitude knowledge requirement is  $10\mu\text{radians}$ , the laser wander certainly could not exceed the corresponding amount of linear travel on the PSD, and ideally should be reduced as much as possible.

Taking the steady state performance data for the diode laser and plotting impact position on the PSM produced the graph below (Figure 9. mm x mm).

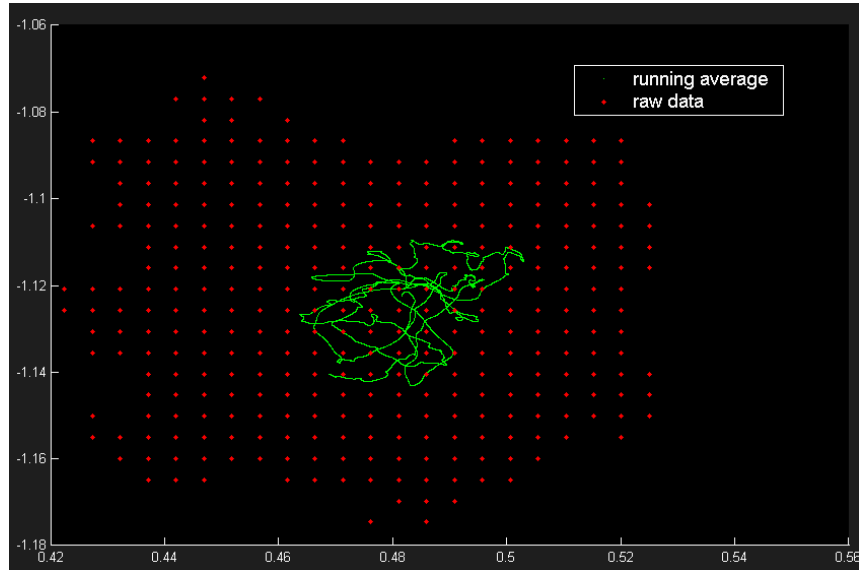


Figure 9. Improving Laser performance – running average

The points in red represent the X and Y co-ordinates collected in the 2000Hz, 60 second sample for PSM1. (Note: At this scale the quantization effect of the analog to digital conversion is obvious, see discussion in section C below.) The spread covered 0.1mm in both the X and Y directions. Over a 4 meter distance this equates to 25 $\mu$ radians of wander; which was insufficient given the pointing requirements. By washing the data through a running average filter (1000 data point running-averaging) the line in green was achieved. By simply averaging-out the aberrant data a stability of 9 $\mu$ radians (0.04mm wander over 4 meters) was achieved. Since the final “star tracker” will be sampling the sensor at 10 to 100 times per second, we can preliminarily extrapolate (possible) sensor accuracy to within 3-4 $\mu$ radians. This estimation has to be verified once the overall sensor is integrated.

### **C. PHASE III – TESTING PSM PERFORMANCE**

The OnTrak PSMs described in Chapter II were also evaluated to ensure suitability for the design. Specifically, tests were run to ensure that the PSMs were capable of providing data for long enough periods, and had the capability to distinguish very fine changes in laser position.

#### **1. Sensor Fatigue**

In order to remove the possibility of sensor error due to fatigue the following series of tests was run. Using the setup described in Figure 2. , The system was started and the laser was run for several hours with one of the PSMs covered to prevent any light from contacting the sensor. After five hours, the cover was removed and a series of high frequency/short duration sensor readings were taken in order to determine if there were significant differences in sensor sensitivity. Figure 10. (below) is a plot of one of these runs. The graph shows that a sensor that has been in operation for hours (the “straight” one) is every bit as sensitive as the “fresh” sensor (listed as the angle sensor). In fact, even in cases where sensors were run for 12 hours the PSMs showed no

tendency to fatigue/lose accuracy. For low power laser operations (2mW and below) the OnTrak PSMs performed just as well after several hours as they did at the beginning.

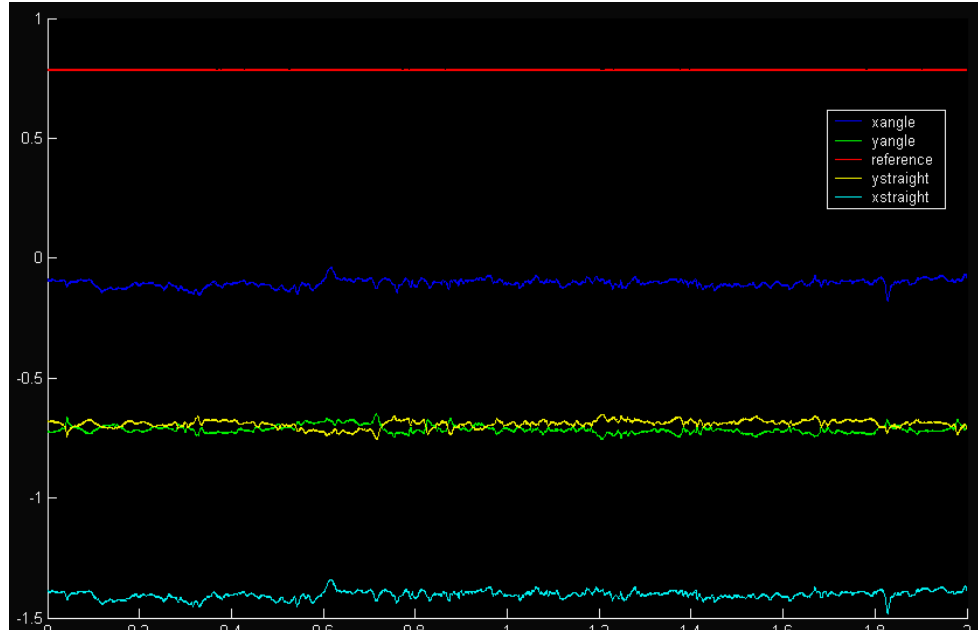


Figure 10. Sensor fatigue test

## 2. Sensor Sensitivity

The OnTrak PSM/amplifier system provides a linear analog output (ranging from -10V to +10V) along the 20mm PSD surface. Since the output is analog (and therefore continuous) the system is, in principle, infinitely accurate. When the analog signal is converted to digital form for processing (a function performed by the Keithley Instruments, Inc KPCI-1802HC PCI board) a quantization error is forced into the signal, limiting sensor accuracy.

Quantization error exists because digital signals cannot replicate analog-continuous signals exactly. Each incoming signal must be broken down into a finite number of divisible sections. Since the KPCI board is capable of 12-bit A/D conversion, this means the 20 volt analog signal ( $\pm 10V$ ) will be divided into  $2^{12}$  sections, each 0.004883V apart. If the actual analog input signal does not exactly match one of these divisions it is rounded off to the nearest one and stored as

that value. This process means that the digital value may be off by as much as 0.002442V (0.004883V÷2). Given this known max error, the system resolution was determined.

The initial signal from the PSM is  $\pm 10V$ , a 20V signal for a 20mm PSD. This means for this system, voltage directly corresponded to location in mm; and laser position is known to within 0.002442mm. Over a 4 meter distance (ref Figure 2. ) this means that a maximum error of:

$$\tan(\theta) = \frac{0.002442mm}{4000mm}$$

$$\theta = \tan^{-1}\left(\frac{0.002442mm}{4000mm}\right) = 0.61\mu\text{radians}$$

would be produced by the sensor system.

Using the data collected during the laser test runs, repeated analysis was run on the input data. Having sorted the data numerically, values were compared in order to determine the distances between values. Removing repeated numbers, six consecutive readings were compared:

Sensor value	
1.42368742368742	}
1.41880341880342	0.00488
1.41391941391941	}
1.40903540903541	0.00488
1.40415140415140	}
1.39438339438339	0.00488
	}
	0.00977

Table 1. PSD sensor readings

Note that in each case the numbers differ by the expected 0.00488 value predicted by the quantization levels (the final number represents 2 x 0.00488; a jump of 2 Q-levels). The PSM/KPCI setup was determined to be more than capable of providing laser position to within 10 $\mu$ radians.

#### D. PHASE IV – TESTING TOTAL SYSTEM PERFORMANCE

After testing the system component-by-component a series of tests were run to determine if the star-tracker modeler as a whole was capable of providing the required  $10\mu\text{radian}$  attitude knowledge.

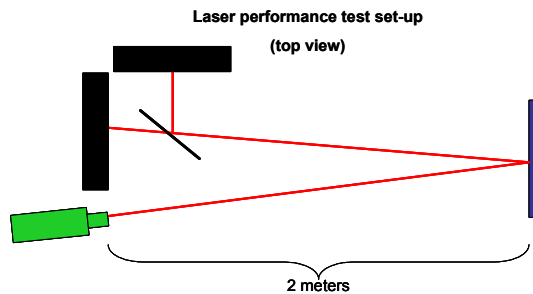


Figure 11. System performance test set-up

Figure 11. above shows the adjusted set-up used to determine system performance. The diode laser (warmed up to steady state operation) was mounted on top of a precision tip/tilt table in order that a pre-determined angle change could be implemented and compared with the resultant change in measured position. The ATT-185-5 precision tilt (pitch-roll) table and ARS-301 precision rotary positioner (see Figure 12. ) manufactured by Aerotech, Inc. were chosen based on the advertised resolution capability of 0.1 arc-second ( $0.485\mu\text{radians}$ ). For detailed information on the Aerotech nano-positioners, see APPENDIX F.



Figure 12. Aerotech, Inc. tip/tilt and rotary position mounts

The geometry of the experiment worked out to be quite simple. Each of the three knobs visible in Figure 12. contain a coarse adjustment and a fine adjustment. The fine adjustment is divided into 32 gradations (circular knob; therefore each gradation represents  $11.25^\circ$  of adjustment). The literature for the devices states that moving the fine adjustment  $0.5^\circ$  will result in 0.1 arc-second of movement (each gradation then equates to 2.25 arc-seconds of movement or  $10.91\mu\text{radians}$  of movement). Over the four meter setup a  $10.91\mu\text{radians}$  adjustment (in tip or rotation) should have been detected as 0.0436mm of movement (tilt was not measured).

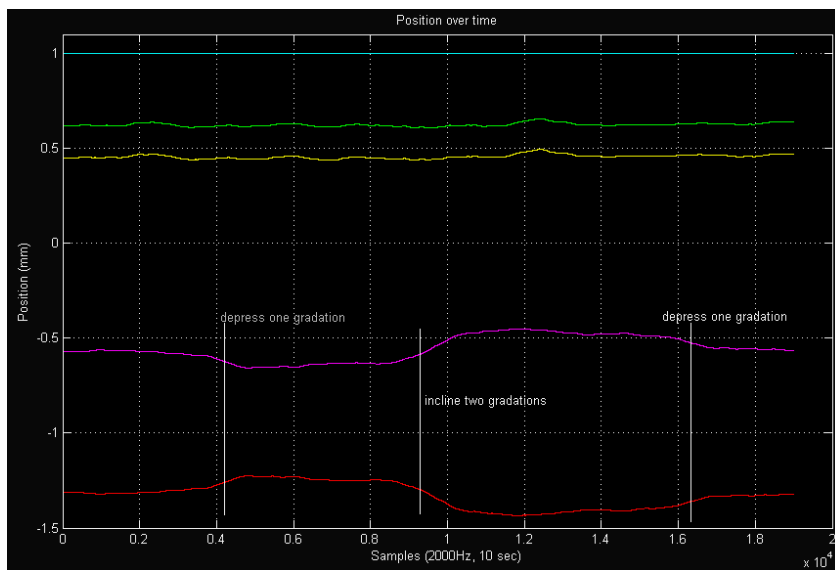


Figure 13. Testing tip-down/tip-up sensitivity

Figure 13 shows the expected trends: tipping down resulted in a change in the Y sense for both PSMs (remember that PSM2 is mounted upside down and shows reverse Y movement) tipping back 2 notches resulted in twice the amount of motion in the opposite direction, and a final depression to the starting position brought the sensors back to their starting outputs. However close analysis of the numerical changes involved gave discouraging results. For every adjustment of one gradation .087 - .089mm of movement was detected in the sensors – approximately double the expected value.

Assuming that the doubling effect came as a result of the mirror, the system was changed (the mirror was removed, and the laser moved to the other side of the table (2 meters from the sensors). The experiments were repeated – with similar results: each movement of the fine adjustment produced twice the amount of sensor reading predicted by the geometry. Several other changes were made to the geometry (moving the laser closer to the sensors and increasing the amount of tip/rotation involved, removing all components except a single sensor and the laser/tip-bed, using two mirrors to determine if optical components were responsible for the doubling, etc.) and in every case the results were the same: each gradation change produced an amount of sensed movement precisely double that which was expected. After discussion with Aerotech technical support, the problem was determined to lie within the Aerotech devices. The devices advertised a 0.1 arc-second resolution for  $0.5^\circ$  fine adjustment – but produced a 0.2 arc-second movement. When the numbers were re-verified using this information the sensors (and the system as a whole) was determined to be functioning properly and accurately.

**THIS PAGE INTENTIONALLY LEFT BLANK**

## IV. SENSOR LAYOUT

To this point, the selection and testing of individual components have been presented, and the capabilities of the sensor as a whole have been examined. This chapter presents the precise layout of the sensor and the incorporation of the design to the testbed itself.

### A. COMPONENT QUANTITIES

In the discussions/analyses above, a consistent design of one laser, two PSMs and a beam splitter has been used. Recall from Chapter III however that the reason two PSMs were used during testing was to remove the possibility of attributing sensor error to laser movement. In the course of all of the experiments run, no discernable PSM error has been detected. For the final design it has been determined that the use of a second PSM is unnecessary and undesirable (each additional PSM used doubles the amount of raw data the onboard processor will have to receive from the sensor).

A single laser directing a beam onto a single PSM is capable of providing the direction of an inertially-fixed vector with respect to a body-fixed frame. In order for the sensor to meet the requirements (provide attitude knowledge to within  $10\mu\text{radians}$  in all 3 primary axes), at least two laser/PSM pairs will be required.

### B. CHOOSING A LAYOUT

The second generation testbed shown in Figure 14. below contains several suitable mounting points for the star tracker modeler (the upper optical equipment deck, the optical equipment deck, the Attitude Control System (ACS) equipment deck and the Automatic Balancing System (ABS) equipment deck). All have standard  $1/4\text{-}20$  holes for mounting the chosen sensor optical equipment. All of these surfaces provide adequate space and appropriate visual access to possible star (laser) locations. The upper optical deck, however, will rotate

independently from the main body, and is therefore not desirable. The optical equipment deck was chosen due to the availability of space, and because it is vibration-isolated from the rest of the testbed.

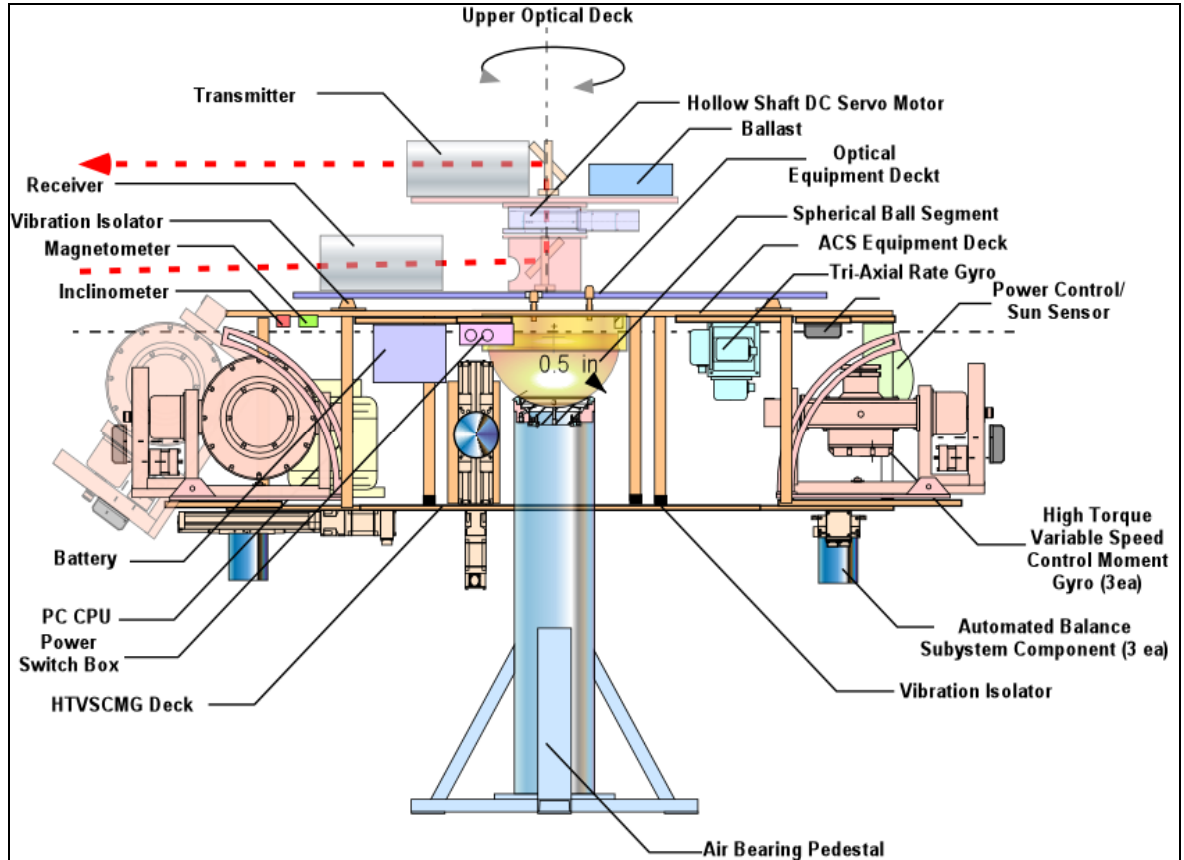


Figure 14. Artist rendition of the NPS Next Generation Testbed

The initial visualization for the final sensor system is shown in Figure 15. This sensor configuration; consisting of three PSMs mounted at  $90^{\circ}$  to each other, was designed to ease the process of converting position knowledge to attitude information (since each sensor shares an axis with each of the other two PSMs redundant data would require no transformation). Closer analysis of the sensor requirements, however, demonstrated that the third PSM was unnecessary. Since each PSM can provide attitude information in two axes; two PSMs can provide three axis information, with one redundant measurement. Further options were explored.

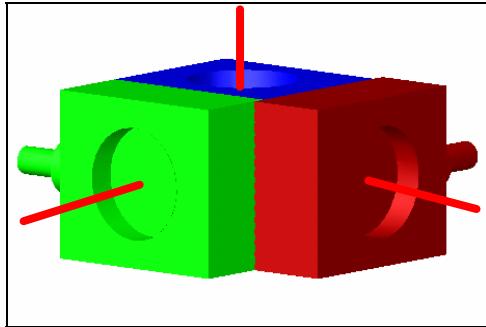


Figure 15. Initial Attitude Sensor configuration

### C. PLACEMENT OF THE PSMS

#### 1. PSMs on Wall

Consideration was given to placing the PSMs on the walls (see Figure 16.). By mounting the small diode laser modules on the platform and directing them to wall mounted sensors position with respect to a reference system could be developed, thus attitude knowledge. This approach had several advantages:

- No need for bus voltage
  - The diode lasers can be powered by 9V batteries
  - The PSMs, amplifiers, and KPCI card could be powered from wall outlets
- No on-board processor (OBP) requirements:
  - Linking the PSMs to a stand-alone computer reduced the loading on the OBP

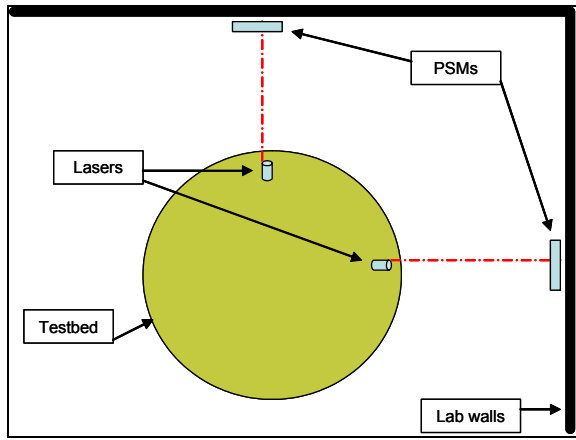


Figure 16. Design consideration one – PSMs on wall

These advantages, however, were not sufficient to overcome the drawbacks of this design. Processing the information on a stand-alone computer meant that a separate wireless link would have to be incorporated. This separate processing and wireless data link would add a time delay to the system that would be very difficult to overcome. However, the primary reason for abandoning a design that placed the PSMs off the testbed was the intent to model the sensor after a star tracker. Quite simply, a star tracker uses ONBOARD sensors to track stars; vice using onboard stars to illuminate inertial sensors.

## 2. Lasers on Wall

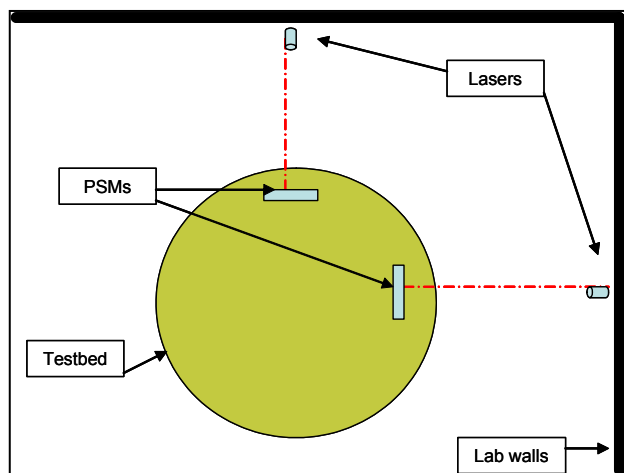


Figure 17. Design configuration two – Lasers on wall

As shown in Figure 17, placing the sensors on the testbed modified the design so that it more closely models a star tracker. Using two lasers and two PSMs attitude knowledge would be known in all three axes (one laser/PSM combination providing table tip/rotation information, the other providing table tilt/rotation information) with redundant angle information for rotation.

### 3. PSM/Laser Arrangement

The decision to place 2 PSMs on the testbed to provide 3-axis knowledge still leaves the issue of what configuration they should be mounted. Figure 18. shows some of the possible design iterations.

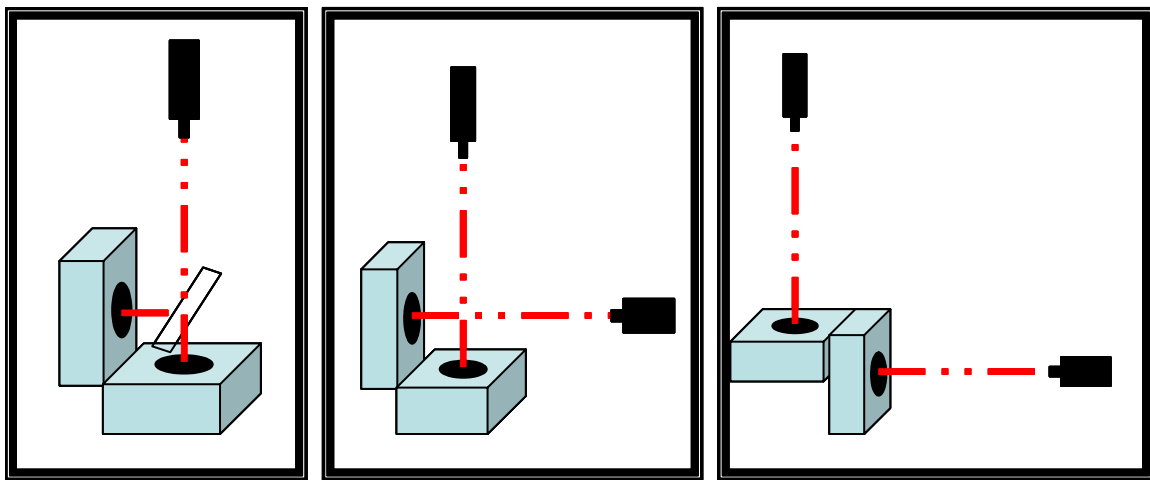


Figure 18. PSM layout considerations

On the left side, the use of only one laser with a beam splitter. This design entails some particularly challenging transformation matrices due to the fact that the single laser means that the axes are coupled. While the issues are not insurmountable, the design was abandoned when the laser test data demonstrated that the selected laser for this application would be less expensive than a beam splitter

The center and right side layouts are simple variations on a theme. The decision to mount the PSMs together (to facilitate getting the PSM surfaces as nearly perpendicular as possible) was very attractive. The final PSM layout

option examined is shown in Figure 17. above. The remaining decision was whether to mount the PSMs together (to facilitate alignment) or to mount the PSMs along the testbed axes. In both cases the PSM would be perpendicular to maximize the reliability of the 3-axis information. Trade studies on the two were just being undertaken when an additional consideration arose that changed the design substantially.

#### **4. Testbed Movement**

As mentioned above, the Optical Equipment Deck was chosen in part due to the vibration isolation. The advantage of this is that the Initial Attitude Sensor will (obviously) be sensitive to table motion, and non-motion vibration would not be discernable from actual table movement. Upon exploration of this theme it was noted that the hemispherical air bearing itself presented a design challenge.

When the table is “down” (meaning when no air is supplied to the bearing) the table has a very stable condition. When floating on the airbearing, however the table height is  $\frac{1}{4}$ ” to  $\frac{5}{8}$ ” higher (due to the air cushion). In either configuration discussed above, this “altitude change” would be interpreted as tip or tilt away from the “star” location.

The solution to this problem was presented by Dr. Nelson Pedreiro and his team at the Lockheed Martin Advanced Technology Center in Palo Alto, CA. In the work conducted by the LM testbed engineering division, a solution to a similar problem has been achieved (see references [10-12]) a very slight variation of which was applied to the NPS testbed, resulting in the configuration shown in Figure 19.

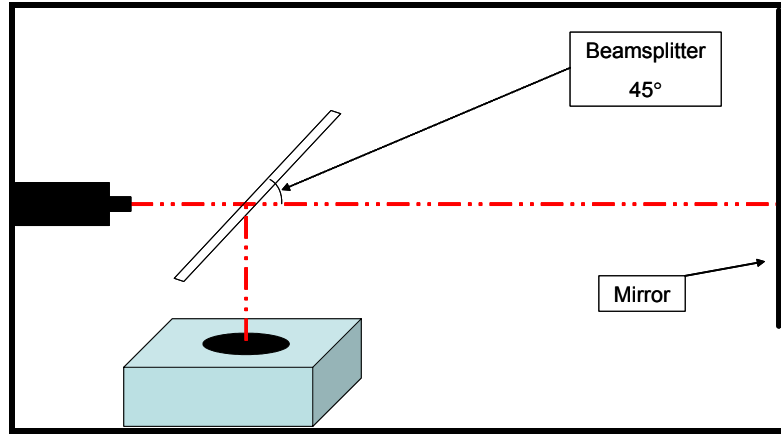


Figure 19. Finalized Sensor design

By mounting the laser, PSM and a beam splitter on the testbed, and using a mirror mounted on the wall, the sensor is immune to the vertical translation caused by the air bearing. Note, since purely vertical translation is not relevant to the testbed motion, it is not necessary to measure it. If the motion is not purely vertical (if some tilt or tip occurs during floatation) this difference WILL be measured by the system. Arguably, the design in Figure 19. does not perfectly model a star tracker (since the “star” is again mounted on the testbed) however the advantages overcome the possible philosophical loss. The beam will still appear from off the testbed (as far as the PSM is concerned) and since the beam is optically doubled in length, the motion of the beam spot is increased without increasing the distance from the laboratory wall, meaning smaller testbed movements will be detectable.

**THIS PAGE INTENTIONALLY LEFT BLANK**

## V. SENSOR KINEMATICS EQUATIONS

As mentioned in previous chapters the ON-TRAK PSMs provide laser point position data in 2 axes (x and y in relation to the PSD centroid). In order to use the PSMs to gather attitude knowledge the “x and y” data taken from the sensors will have to be converted into tip/tilt/rotation information.

Since the starting point of the laser beam (the “star”) is known with respect to the body frame, and the end-point position of the beam is measured by the PSM (a zero measurement corresponding to an inertially fixed position) a vector can be computed for each sensor set. Several methods of determining attitude from known vectors have been explored [13-15]. For the NPS testbed, the deterministic approach [16] was used. The position of the beam spot on the PSM is a direct result of the angular position of the testbed. Any tip( $\Theta$ ), tilt( $\alpha$ ) and/or rotation( $\gamma$ ) causes a corresponding change in the PSM measured position of the beam. Once this relation is calculated  $\Theta$ ,  $\alpha$ , and  $\gamma$  can be calculated from any set of PSM observations.

### A. RELATING BEAM POSITION TO ROTATION

Figures 20 and 21 below show the layout of one of the star tracker modelers. There are 2 units (one along the testbed X axis, one along the testbed -Z axis) however the layout of each is identical. Both units measure rotational movement and the proof for each is the same.

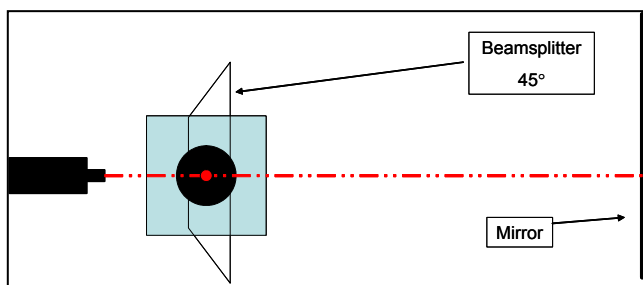


Figure 20. Sensor layout – Top view

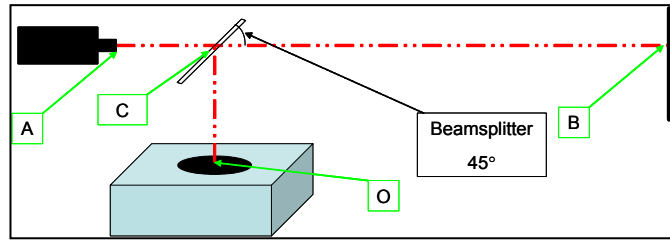


Figure 21. Sensor layout – Side view

It is important to note that the laser, the PSM and the beam splitter are fixed in place on the testbed. This means that changes to the testbed position also move these components. For example, if the table is rotated  $\gamma$  degrees (see Figure 22. below) the laser, PSM and beam splitter are also rotated  $\gamma$  degrees.

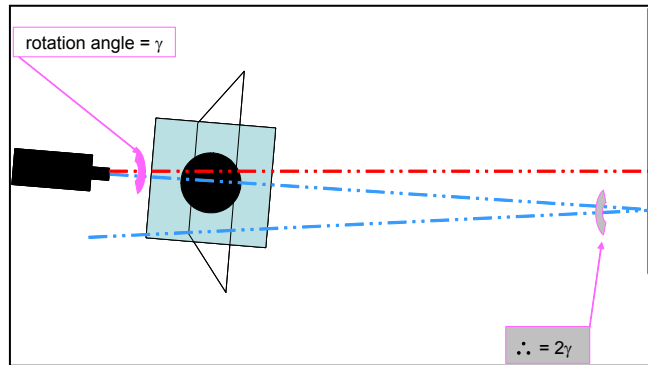


Figure 22. Testbed rotation and sensor movement

This simplifies the geometry significantly. As the PSM/beam splitter fixed pair rotate the beam point travels along the X-axis of the PSM (see figures 23 and 24 below). For purely rotational movement there is no change detected in the PSM Y-axis. Because of this it is possible to relate a change in the detected position of the laser beam along the PSM X-axis directly to a rotation of the testbed.

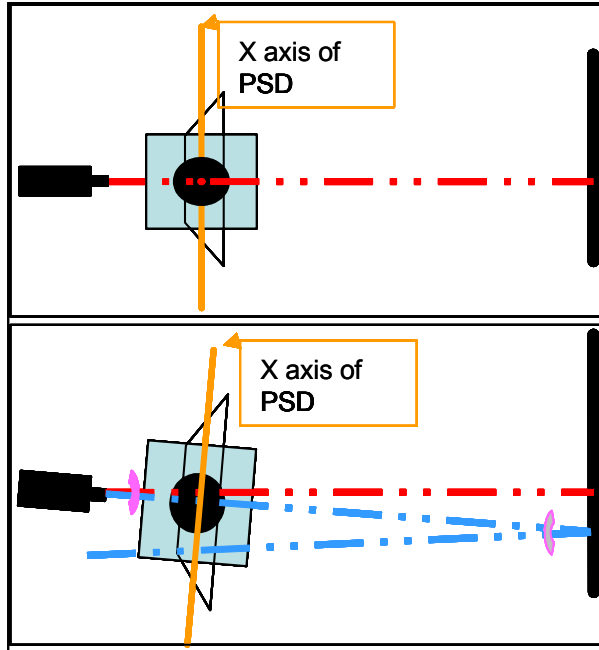


Figure 23. Rotation effect on PSD X-axis

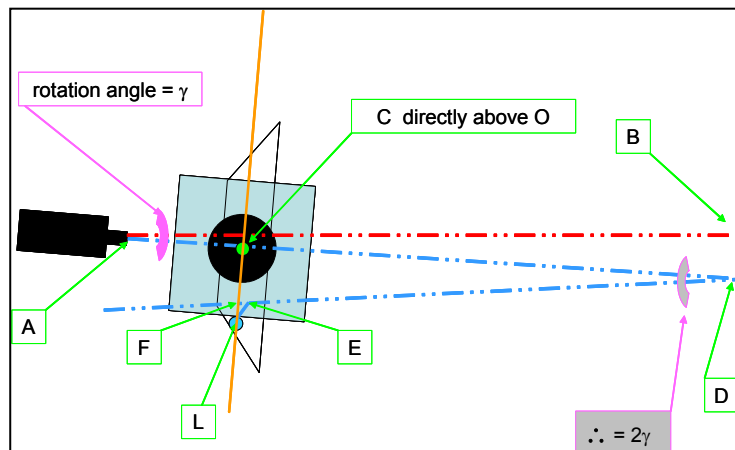


Figure 24. Star tracker model kinematic derivation points (rotation).

The following list explains the letters/points shown in Figures 21 and 24.

- A Point where beam leaves laser
- B Point where beam hits mirror when  $\gamma=0^\circ$
- C Point where beam first contacts the beam splitter.  
Note: this is a constant due to the fact that the beam splitter, laser and PSD are hard-mounted together.  
Thus,  $C_{\text{initial}}=C_{\text{final}}$  or  $C_{\gamma=0^\circ}=C_{\gamma\neq0^\circ}$
- D Point where beam hits mirror when  $\gamma\neq0^\circ$
- E Second point where the laser contacts the beam splitter (different from C if  $\gamma\neq0^\circ$ )

O	The center of the detector. Note that our initial setup will require that the beam will contact the PSD at O when $\gamma=0^\circ$ .
L	The point where the beam impacts the detector when $\gamma \neq 0^\circ$
h	The height of the beam splitter above the PSD (aka $\overline{OC}$ )
F	Conceptual point on the X axis, directly beneath point E
$\overline{OL}$	The key vector. $\overline{OL} = \Delta X$ (the change in PSM X-axis reading due to $\gamma$ )
$\overline{CO}$	A vector of known magnitude (by design)
$\overline{AB}$	A vector of known magnitude (by design)
$\overline{AO}$	A vector of known magnitude (by design)
$\gamma$	The amount angular rotation of the platform with reference to the zero position

Statements	Proofs
$\overline{AD} = \frac{\overline{AB}}{\cos(\gamma)}$	
$\overline{CD} = \frac{\overline{AB}}{\cos(\gamma)} - \overline{AC}$	$\overline{CD} = \overline{AD} - \overline{AC} = \frac{\overline{AB}}{\cos(\gamma)} - \overline{AC}$
$\overline{CE} = \left( \frac{\overline{AB}}{\cos(\gamma)} - \overline{AC} \right) \tan(2\gamma)$	$\overline{CE} = \overline{CD} \tan(2\gamma) = \left( \frac{\overline{AB}}{\cos(\gamma)} - \overline{AC} \right) \tan(2\gamma)$ $\angle DCE$ is a right triangle
$\overline{FL} = h \tan(2\gamma)$	$\overline{EL}$ is a downward projected beam from the beam splitter. Consider the right triangle $\Delta EFL$ $\overline{EF} = \overline{CO} = h$
$\Delta X = \tan(2\gamma) \left( h + \frac{\overline{AB}}{\cos(\gamma)} - \overline{AC} \right)$	$\Delta X = \overline{OF} + \overline{FL}$ $\Delta X = \overline{CE} + \overline{FL}$ $\Delta X = \left( \frac{\overline{AB}}{\cos(\gamma)} - \overline{AC} \right) \tan(2\gamma) + h \tan(2\gamma)$ $\Delta X = \tan(2\gamma) \left( h + \frac{\overline{AB}}{\cos(\gamma)} - \overline{AC} \right)$

Table 2. Developing the rotational kinematics

Thus, the equation relating PSD X-axis reading to testbed rotation is:

$$\Delta X = \tan(2\gamma) \left( h + \frac{\overline{AB}}{\cos(\gamma)} - \overline{AC} \right)$$

Where all quantities are constant except  $\Delta X$  (given by the PSM) and  $\gamma$  (which is the desired rotation angle). For small angles (the field of view of the sensor will be less than  $2^\circ$ ) the relationship between  $\Delta X$  and  $\gamma$  is nearly linear (see Figure 25).

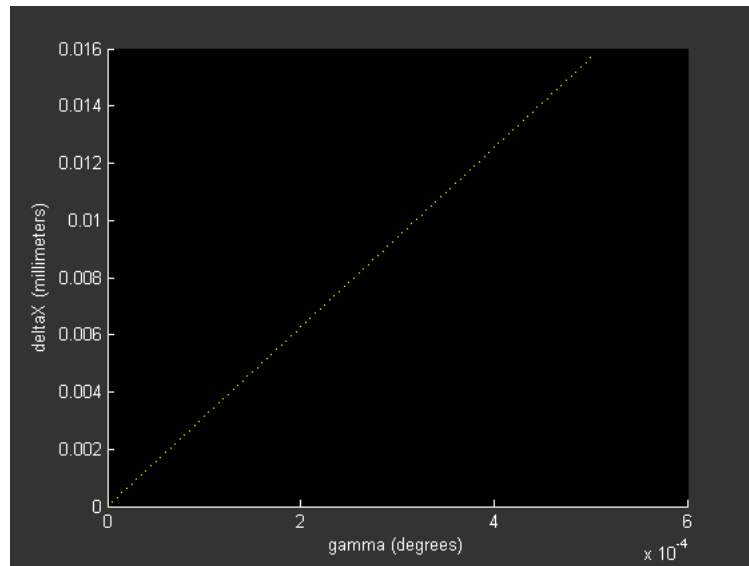


Figure 25.  $\Delta X$  vs.  $\gamma$  for small angles

## B. RELATING BEAM POSITION TO TIP/TILT

The star tracker modeler measures tip and tilt using separate laser/beam splitter/PSM units; one mounted along the testbed X axis [measuring tip( $\Theta$ )] the other along the testbed  $-Z$  axis [measuring tilt( $\alpha$ )]. The derivation of the kinematics is the same for both cases, however, as the motion experienced is the same.

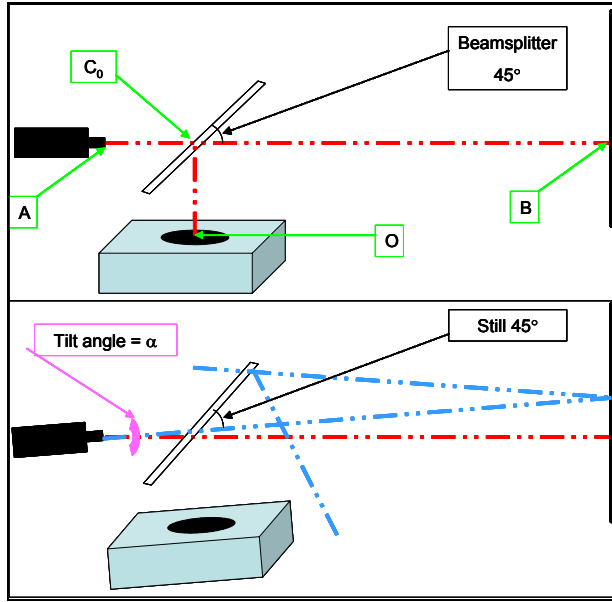


Figure 26. Star tracker modeler during testbed tilt

As shown in Figure 26, testbed tilt causes the beam reflected by the mirror to come back to the beam splitter at a different position. This means the downward reflected portion of the beam will contact the PSM at a different location. (The contact point is still along the PSM Y-axis however.) Similar to the derivation for rotation above it is possible to geometrically link a change in measured PSM Y-axis position directly to testbed tilt. (Note that for clarification the angles have been exaggerated to the point that the beam is shown off the sensor. The Kinematics are valid for any angle, however the sensor is only large enough to detect small angles.)

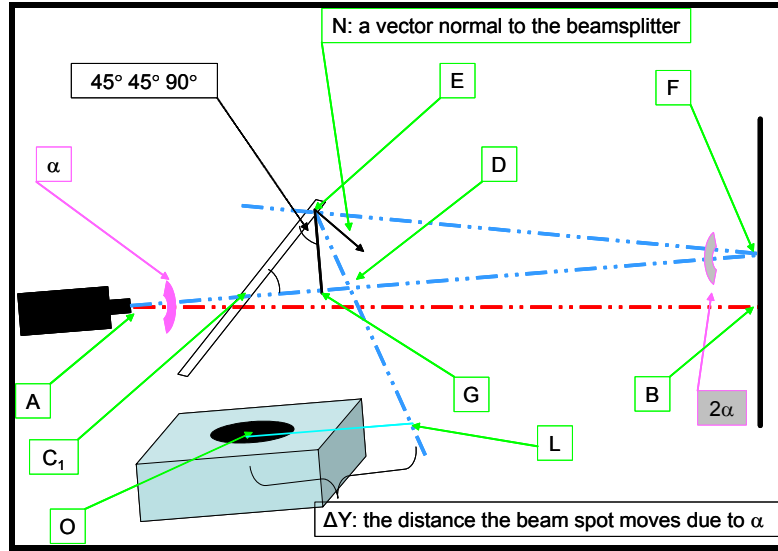


Figure 27. Star tracker model kinematics derivation points(tilt/tip)

- A Point where beam leaves laser
- B Point where beam hits mirror when  $\alpha=0^\circ$
- C Point where beam first contacts the beam splitter. Note: this is a constant due to the fact that the beam splitter, laser and PSD are hard-mounted together. Thus,  $C_0=C_1$  even though these points appear different in the drawings.
- D The point of intersection of  $\overline{AF}$  and  $\overline{EL}$
- H A point on the PSD representing an extension of  $\overline{EG}$
- O The center of the detector. Note that our initial setup will require that the beam will contact the PSD at O when  $\alpha=0^\circ$ .
- L The point where the beam impacts the detector
  
- $\overline{EN}$  A vector normal to the beam splitter at the second laser contact point
- $\overline{EG}$  A vector which forms one side of a  $45^\circ 45^\circ 90^\circ$  triangle ( $\Delta EGC_1$ )
- $\overline{OL}$  The key vector.  $\overline{OL} = \Delta Y$  (the change in PSM Y-axis reading due to  $\alpha$ )
- $\overline{CO}$  A vector of known magnitude (by design)
  
- $\alpha$  The change in elevation of the platform with reference to the zero position
- $\beta$  Angle of incidence/reflection at beam splitter at the second laser contact point.

Statements	Proofs
$\angle DEG = 45^\circ - \beta$	$\angle NEG = 45^\circ$ by design $\angle DEG = \angle NEG - \beta$
$\beta = 45^\circ - 2\alpha$	Consider the right triangle $\Delta EGF$ $\Delta EGF \rightarrow \angle FEG + \angle EGF + \angle GFE = 180^\circ$ $\Delta EGF \rightarrow (45^\circ + \beta) + (90^\circ) + (2\alpha) = 180^\circ$ $\Rightarrow \beta = 45^\circ - 2\alpha$
$\therefore \angle DEG = 2\alpha$	
$\overline{AF} = \frac{\overline{AB}}{\cos(\alpha)}$	
$\overline{CF} = \overline{AF} - \overline{AC} = \frac{\overline{AB}}{\cos(\alpha)} - \overline{AC}$	
$\overline{CE} = \frac{\sin(2\alpha)}{\sin(135^\circ - 2\alpha)} \overline{CF}$	sines Consider the right triangle $\Delta CFE$ and apply law of sines $\frac{\sin(90^\circ + \beta)}{\overline{CF}} = \frac{\sin(2\alpha)}{\overline{CE}} \Rightarrow \frac{\sin(90^\circ + 45^\circ - 2\alpha)}{\overline{CF}} = \frac{\sin(2\alpha)}{\overline{CE}}$
$\overline{OH} = \overline{CE} \cos(45^\circ)$	$\overline{OH} = \overline{CG}$
$\overline{HL} = (\overline{CG} + \overline{CO}) \tan(2\alpha)$	$\overline{HL} = (\overline{EH}) \tan(2\alpha)$ $\overline{HL} = (\overline{EG} + \overline{GH}) \tan(2\alpha)$ $\Delta EGC_1$ is an isosceles triangle $\overline{HL} = (\overline{CG} + \overline{CO}) \tan(2\alpha)$
$\Delta Y = \overline{OL} = \overline{OH} + \overline{HL} = \overline{CE} \cos(45^\circ) + (\overline{CG} + \overline{CO}) \tan(2\alpha)$ $\Delta Y = \overline{CE} \cos(45^\circ) + (\overline{CE} \cos(45^\circ) + \overline{CO}) \tan(2\alpha)$ $\Delta Y = \overline{CE} \cos(45^\circ) + \overline{CE} \cos(45^\circ) \tan(2\alpha) + \overline{CO} \tan(2\alpha)$ $\Delta Y = \overline{CE} \cos(45^\circ)(1 + \tan(2\alpha)) + \overline{CO} \tan(2\alpha)$ $\Delta Y = \left( \frac{\sin(2\alpha)}{\sin(135^\circ - 2\alpha)} \overline{CF} \right) \cos(45^\circ)(1 + \tan(2\alpha)) + \overline{CO} \tan(2\alpha)$ $\Delta Y = \left( \frac{\sin(2\alpha)}{\sin(135^\circ - 2\alpha)} \right) \left( \frac{\overline{AB}}{\cos(\alpha)} - \overline{AC} \right) \cos(45^\circ)(1 + \tan(2\alpha)) + \overline{CO} \tan(2\alpha)$	

Table 3. Developing the tip/tilt kinematics

Thus, the equation relating PSD Y-axis reading to testbed tilt is:

$$\Delta Y = \left( \frac{\sin(2\alpha)}{\sin(135^\circ - 2\alpha)} \right) \left( \frac{\overline{AB}}{\cos(\alpha)} - \overline{AC} \right) \cos(45^\circ) (1 + \tan(2\alpha)) + \overline{CO} \tan(2\alpha)$$

As before, the only unknowns are  $\Delta Y$  (measured by the PSM) and  $\alpha$ , the tilt measurement desired. Again, for small angles the relationship between  $\Delta Y$  and  $\alpha$  is nearly linear (see Figure 28).

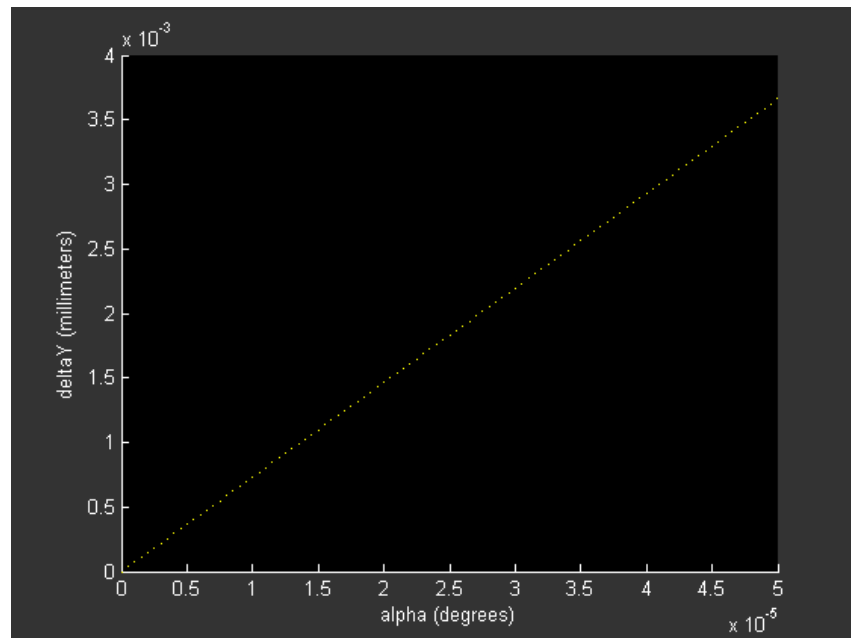


Figure 28.  $\Delta Y$  vs.  $\alpha$  for small angles

**THIS PAGE INTENTIONALLY LEFT BLANK**

## VI. TESTBED/SENSOR SETUP

This chapter will serve primarily as documentation for the procedure of positioning the attitude sensor, should it be necessary in the future to replace/re-align any components.

### A. EQUIPMENT USED

- Tape Measure (metric if possible)
- 4' level
  - Note: a long level is necessary because the Optical Equipment Deck is not flat. If a small bubble-type level is used the table may not be level. Use a long builder's style level laid across the entire surface.
- Pencil
- Large Triangle (90° square)
- LaserMark® MP5 Five-Beam Laser (See APPENDIX G)
- A magnetic Polycast® Protractor (See APPENDIX H)

The LaserMark® MP5 Five-Beam Laser is a device used primarily in construction. It contains 5 laser beams, all arranged at 90° angles. Three of the beams are in the horizontal plane, one points up, the final points down. The beams are spaced around a shared origin so that when turned on, five beams emanate from the device providing an automatic reference system. Additionally the device is self-leveling so that minor inclinations are compensated for.

### B. STEP ONE – CALIBRATE THE MP5

Performed in accordance with the operator's manual to ensure maximum accuracy; this procedure occurred in the hall outside the Optical Relay Mirror Laboratory. This hall crossway allowed distances of 50m x 35m to be used for calibration. In summary, the MP5 was placed on the tripod and centered over a mark on the floor. The 3 horizontal beams were aligned so that one traveled the 50 meter length of the hallway, one traveled 25 meters down the crossway, and the other the 12 meters to the doors. The location of each beam spot was marked on the wall it contacted. By carefully rotating the MP5 90° until one of the beams was in a spot previously occupied by its predecessor, the location of the

other 2 beams were checked to ensure they fell on a prior beam spot. If the beams failed to fall on a mark, the set screws were adjusted (according to the owner's manual). When a series of 90° rotations bring the beams constantly into the same location, the unit is properly calibrated and is ready for use.

### **C. STEP TWO – POSITION TABLE**

The table was positioned so that the edge of the optical equipment deck was 2 meters away from the West wall, and 2 meters from the South wall. The 2 meter distance was chosen primarily to ensure the sensor had an optical path greater than 4m, but also to allow sufficient working space around the test bed.

### **D. STEP THREE – REMOVE UPPER OPTICAL EQUIPMENT DECK**

The Upper Optical Equipment Deck was removed in order to clear the optical equipment deck as much as possible to facilitate the sensor installation/alignment/calibration. This was necessary because the table axes had not been clearly identified and marked. If the axes had been marked, steps four and five would not have been necessary (if the sensor is being re-aligned, and the axes are still clearly indicated, skip to Step 5).

### **E. STEP FOUR – FIND THE TABLE CENTER**

The hole in the center of the Optical Equipment Bench was covered with a piece of sheet metal (affixed to the surface with 1/4-20 bolts so that it would not move).

- a. Using a tape measure, one end was placed at the Optical Equipment Deck edge and the opposite edge of the table was found by noting the max distance between the two points (circular table, therefore the max distance between points on the edge is on a line over the center). The line along the edge of the tape was marked.
- b. The tape measure was shifted to another point, and another line drawn.
- c. Repeat as necessary until a clear center point is determined.

- d. Note that the point where the majority of the lines intersect is the table center. Some lines will not cross this point due to irregularities in the roundness of the deck.

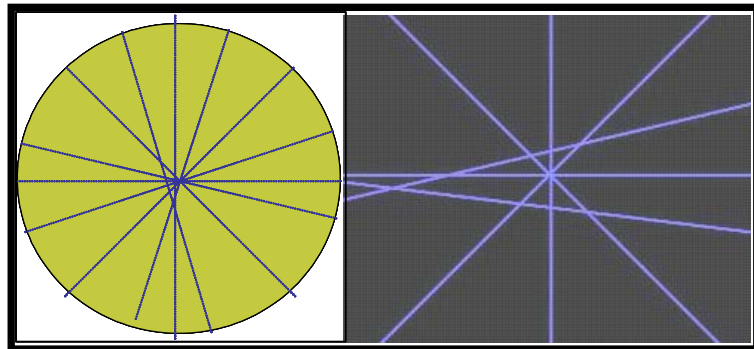


Figure 29. Finding table center

## F. STEP FIVE – INERTIAL REFERENCE SYSTEM

For our simulator, the star tracker modeler will provide attitude information with respect to an “inertial” reference frame. To simplify the transformation matrix, it was decided to define this inertial frame to coincide with the table reference frame (when the table is at the zero position). Thus, the center point that was found for the table will also be the axial center point of the inertial reference frame.

### 1. Tape Measure Estimation

The location of the Inertial reference points (the marks on the walls that define the inertial reference frame) were estimated:

- a. See Figure 30; since the center is 60 cm from the optical equipment deck edge, and the edge is set 200cm from the W and S walls, the inertial reference X and  $-Z$  points were estimated\* to be 260cm from the SW corner.

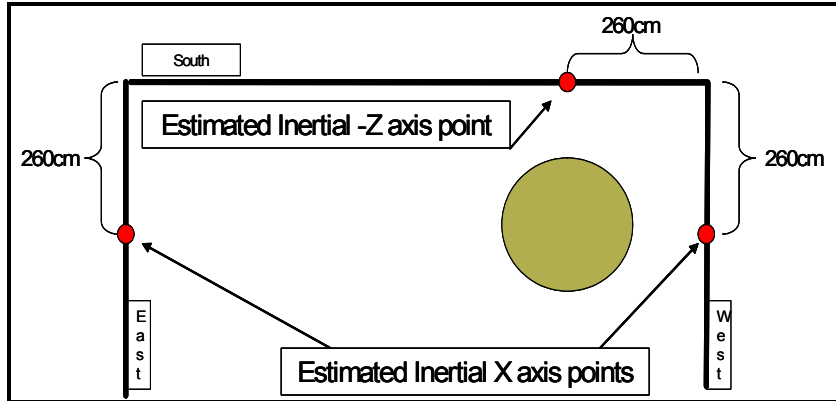


Figure 30. Inertial point estimation

- i. \*Caution should be taken not to attempt to determine the inertial reference frame using only a tape measure and the walls, as the walls are NOT GUARANTEED to be square. In the following sections this estimation is adjusted
- b. Similarly, the  $-X$  point was estimated on the East wall, and the  $Z$  point on the North wall.

## 2. MP5 Correction and Verification

- a. Correction
  - i. The MP5 comes equipped with a 3" high tripod which allows the user to suspend the unit over a designated point. The laser tool was placed over the table center point (the Inertial Y axis, and the table Y axis) and one of the 3 horizontal lasers was aligned with any one of the estimated axis points (in our example the  $+X$  point was used).
  - ii. After allowing the MP5 to settle, the  $-Y$  axis point was checked to see that it was  $90^\circ$  off of the  $+X$  point. The estimated point was NOT  $90^\circ$  (see Note, above) and the placement of the axis point was corrected.
  - iii. This step was repeated for the  $-X$  and  $+Y$  points.
- b. Verification
  - i. By spinning the MP5  $90^\circ$  and allowing the unit to settle; the lasers should correspond exactly with the points, confirming that the inertial reference frame axes are precisely perpendicular.
  - ii. By performing the  $90^\circ$  spin repeatedly the axes were verified. (If the marks and the lasers do not agree, re-calibrate the MP5 and repeat step (2).)

The procedure outlined above provided a series of inertial axial points. By raising the MP5 3" and repeating the procedure a second set of points in the  $\pm X$  and the  $\pm Z$  directions was provided. Using the large triangle (90° square) the two  $+X$  points were connected with a line, and the two  $-X$  points with a line. These lines are both contained within the Inertial XY plane. Connecting the  $+Z$  points, and the  $-Z$  points defined the ZY plane.

Before moving on to step 6, one more set of inertial axes indicators needed to be laid out – directly over the testbed. These marks (an X and Z axes plane) are necessary for aligning the beam splitters.

1. The MP5 was placed (on its tripod) at any point along the table X-axis (or Z-axis). [Note that when the unit is positioned correctly (when the downward laser is properly centered on the table axis) there is a beam spot on the ceiling DIRECTLY over that axis.] This spot was marked.
2. Moving the MP5 along the axis several spots were marked on the ceiling.
3. Using the 4-foot builder's level as a straight edge, the points were connected to form an X-Z plane with an origin along the Y axis.

The overhead markings will also be beneficial in enabling an operator to re-align the testbed to the inertial frame after the testbed-top has been moved.

1. Level the testbed.
2. Place the MP5 at any point along the testbed X or Z axis and (keeping the table level) rotate the table until the MP5 is illuminating both the Table axis (downward) and the Inertial axis (on the ceiling).
3. Verify correct alignment by moving the unit around to different locations on the testbed axes and confirming alignment with the ceiling reference system.

## **G. STEP SIX – ALIGN THE TESTBED TO THE INERTIAL REFERENCE FRAME**

Note: ensure the testbed is level when performing this step.

By design, the reference frames share a common center point. To align the frames, the MP5 was positioned off the table but in the Inertial XY plane (the beam should be approximately 3-4" above the table surface), as shown in Figure 21 below. If the inertial reference system was created correctly, the beam should

cross the table exactly at the center point. The table was rotated so that the table X axis was aligned with the beam.

(To facilitate this, the table X axis should be clearly marked on the upper surface.) Using the large triangle (90° square), position the table so that the square (when placed anywhere along the axis mark on the table surface) also contacts that laser beam.

#### 1. Notes:

- a. if the table surface is uneven, this may take several attempts (similar to finding the table center)
- b. if the testbed is not level, this procedure will not work

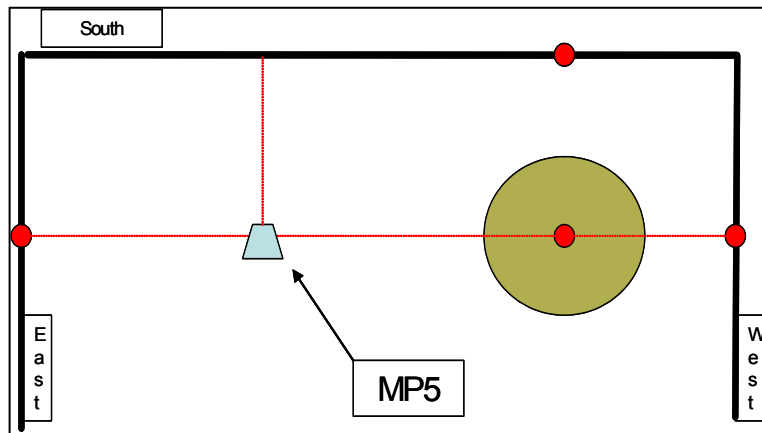


Figure 31. Aligning the table to the inertial axis

\*\*It is not possible using the equipment described to exactly align the 2 reference frames (keeping in mind  $\mu$ -radian accuracy requirements); however caution should be taken to get the alignment as close as possible. The closer the 2 frames are during sensor installation, the easier the correction matrix will be to create.

Move the MP5 to a position in the YZ Inertial plane approx 3" above the testbed and repeat to verify the alignment of the table ZY plane. When completed, the inertial axes and the test bed axes are aligned.

## **H. STEP SEVEN – INSTALL POSITION SENSING MODULES**

Close examination of the ON-TRAK PSMs will show that while the PSD is positioned off-center within the protective case; the PSD center is clearly marked on the outside of that case. Using these marks and the 90° square, the PSM was positioned on the table centered above the axis (one unit along the X-axis, one along the -Z-axis). This aligned the axis of the PSD with the testbed axis. The center of the PSD was placed 7cm from the edge of the Optical Equipment Deck – the amount of distance is not critical, however it is very important to be precise in measuring this distance for use in the calculations in Chapter VI. In other words placing the unit 6, 8 or even 10 cm from the table edge would have worked; as long as the distance was known accurately. On the NPS testbed 7cm was chosen because it facilitated the placement of the beam splitters. Note: when the PSMs are correctly mounted measure the distance from table center to the center of the PSD (this number will be needed when aligning the beam splitters)

The ON-TRAK PSMs have a procedure for calibrating the unit in the event that a laser spot directed to the exact center of the PSD gives a non-zero reading. This step (if necessary) will be the final step taken in this chapter.

## **I. STEP EIGHT – INSTALL THE DIODE LASERS**

Just as in step seven, the placement distance of the laser diode (along the axis) is not critical as long as accurate measurements are taken. The NPS testbed lasers were placed 18cm from the edge of the deck.

### **1. FOCUS**

Using a mirror temporarily placed at the wall (in the position the star tracker modeler mirror will be); the laser was reflected back to the table and focused at a distance corresponding to the total path length. This distance is the distance from the laser cavity to the mirror, directly back to the PSD center and down. In Figure 32 (below) the path length is shown as A→B→C→O.

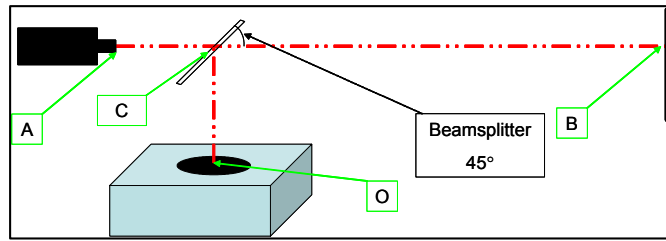


Figure 32. Path length

## 2. Align with Respect to Inertial

Placing the MP5 back in the center of the table (on the tripod) the temporary mirror installed above was removed. The unit was aligned to the inertial system and the table axis was checked to ensure that it was still aligned to the inertial frame. The diode laser was positioned so that the MP5 laser crossed directly over the center of the diode cavity and the diode laser directed so that it shined onto the wall inertial reference mark put down in step five. Figure 33 below shows a “gun-site view” of the diode laser. In the foreground the bottom of the MP5 laser contacts the center of the diode laser cavity while the remaining portion of the MP5 laser continues on to the inertial reference mark on the wall. Below that point the diode laser spot can be seen.

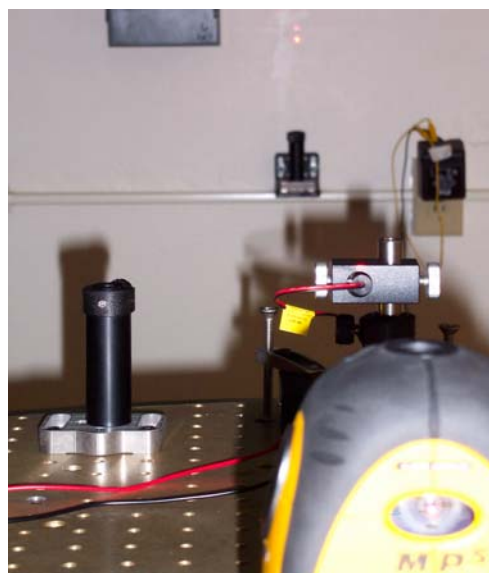


Figure 33. Gun-site view of diode laser alignment

The beams were then checked to ensure they were parallel. Since the MP5 laser system includes an auto-leveling device, the reference beam is parallel to the axes (testbed and inertial). The 90° square was used to verify that at the diode laser cavity (point A in Figure 32) the beams were both correctly centered above the testbed Z-axis. While performing this step, the square was marked with the location (height) of each beam. Since the beams need to be parallel, this distance should be the same at any point in the optical path. By adjusting the diode laser as necessary, it was ensured that the diode laser path was directly over the axis and parallel to the reference beam. The use of a semi-transparent (see Figure 34) material made the process of checking parallel distance easier.



Figure 34. Semi-transparent 90° square

#### **J. STEP NINE – INSTALL THE WALL MIRRORS**

The use of optical components mounted in adjustable holders greatly simplified the alignment process. The wall mirror and beam splitter (see Appendices I and J) mountings allow manual adjustment of a beam in the general direction desired; from there the fine adjustment mechanisms can be used to steer the beam into place.

The mirrors were positioned so that the diode laser beam made contact  $\frac{1}{4}$ " to  $\frac{5}{8}$ " below the center of the mirror (this distance corresponds to the amount of table "lift" generated by the air bearing). The mirrors used for the NPS testbed measure 50mm (square) whereas the PSDs themselves are 20mm x 20mm.

Because of the geometry of the situation, the mirrors are much larger than is strictly necessary (as the table rotates, the beam will leave the surface of the PSD before it leaves the surface of the mirror). If smaller mirrors are used, more careful calculation of the testbed height change would have to be performed to ensure maximum field of view (FOV) of the sensor.

Fine adjustments were made to the mirror so that the laser diode beam was reflected directly back into its own cavity. If step nine (above) was correctly performed, the MP5 laser should also be reflected back into its cavity.

#### **K. STEP TEN – INSTALL THE BEAM SPLITTERS**

Since the beam splitter holder has three adjusters, it would be very difficult to position the device into the exact correct position using the magnetic Polycast® Protractor alone. In fact, depending on how the beams splitter is mounted it may not be possible to correctly align it at all using a protractor. This is the reason the measurement was taken in step seven (the distance from the center of the PSD to the table center). Using this distance, a mark was made on the ceiling axes above the PSD center.

The beam splitter was then positioned over the PSM ensuring that the alignment was as close as possible using the protractor to ensure a 45° angle. The height was set so that the diode laser beam cut through the center of the beam splitter. [If the alignment is even close two beam spots should now be visible: one on the PSD and one on the ceiling (near the mark just placed on the axis.)] Using the fine adjustments on the beam splitter holder these spots were steered exactly on center (one to the PSD center, one to the ceiling mark).

If the light reflected upward hits the ceiling axis on the indicated point, and the reflected beam spot on the PSD is in the center, the beam splitter must be in the correct position.

To verify the correct placement of the beam splitters, note that the upward reflected beams from the X-axis beam splitter, the -Z-axis beam splitter and the

MP5 must all be parallel. Measure the distance between each and verify that distance at several points between table height and ceiling.

#### **L. STEP ELEVEN – CALIBRATE THE PSMS**

Now that the star tracker modeler is in place, it is important to verify the calibration of the PSMs. Note that this step is different from the system calibration (discussed in CH VII); here ONLY the PSMs are calibrated. This is necessary due to the photosensitive nature of the PSDs and the lighting configuration of the lab. The procedure for calibration is outlined in the ON-TRAK OT301 amplifier user's manual. However, before beginning to calibrate these devices it is important to note that lighting conditions will matter. Since the star tracker modules use photosensitive diodes any alteration in lighting conditions will affect the sensor readout. In the NPS Optical Relay Mirror Lab, there are six light switches controlling the fluorescent lighting for the overhead lights. If the calibration is performed in a given lighting condition, it is critical the system be run in this same condition. To this end (and to protect the alignment of the optical train) a cover was incorporated.

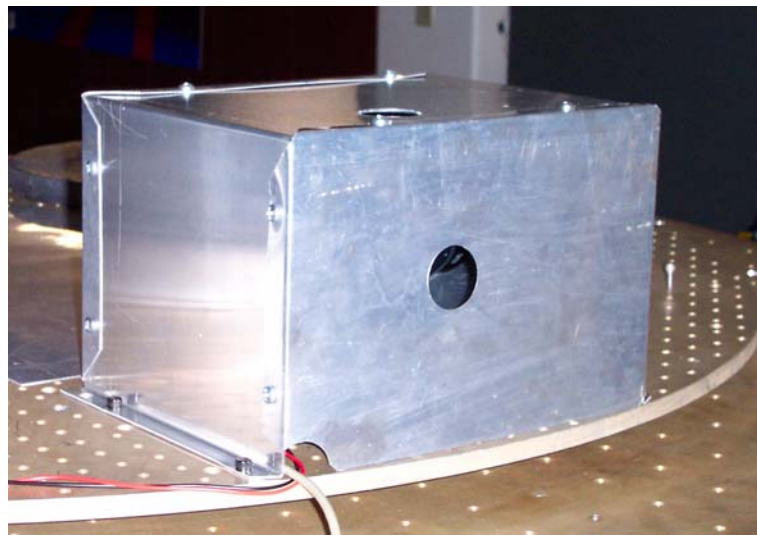


Figure 35. Optical train cover

A cover such as this (see Figure 35 above) provides alignment protection for the optics (to prevent an inadvertent “bumping” that may require several hours of Chapter V re-work) and also encloses the sensor unit to prevent fluorescent lighting interference. Filters are also a viable option (choosing a 635nm bandwidth discriminating optical filter) and would ensure that only the frequency of interest could be interpreted by the sensor. With an appropriate optical screen in place, the PSM calibration knob was adjusted to read zero (or as close as possible) on both axes (for each unit).

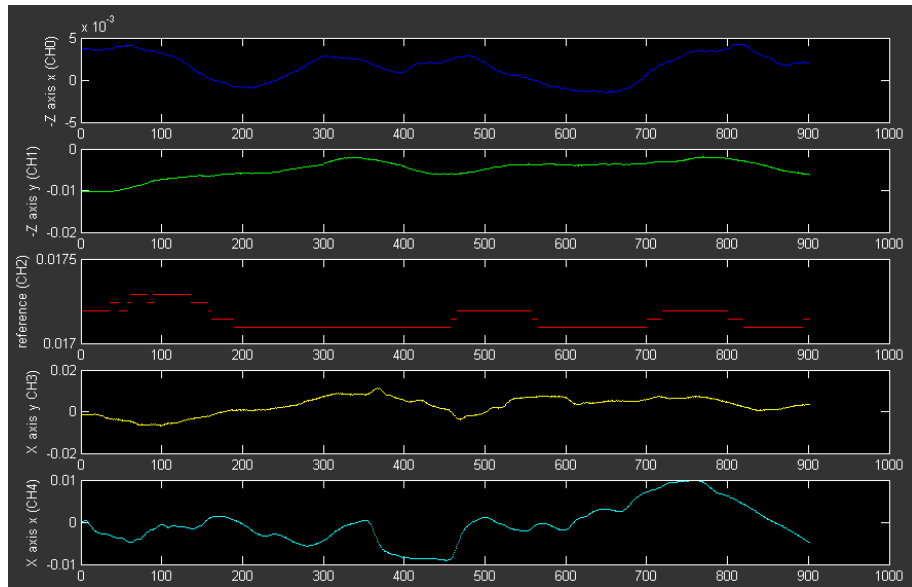


Figure 36. Post calibration sensor readings (mm vs. # of samples for 10 seconds )

Figure 36 shows the result of the PSM sensor readings after calibration. The maximum error in a static (testbed not floating) reading is 0.015 mm. Given the geometry of the unit this equates to a (maximum)  $3.7\text{-}\mu\text{radian}$  error. This error is due to the wander associated with the diode laser.

The Star Tracker sensor is now installed, aligned and ready for calibration.

## VII. SENSOR CALIBRATION

In spite of all the care taken in setting up the sensor, the alignment WILL be off. When dealing with micro-radians, proper alignment using tape measures and protractors is simply not possible. Similarly, misalignments occur in spacecraft mounted star trackers as well [16].

The  $1\sigma$  star tracker accuracy is 6 arc-s in the cross boresight axes and 37 arc-s in the boresight axis.<sup>3</sup>

During the complete testbed system integration an Alignment Kalman Filter (AKF)<sup>4</sup> will be used to correct for misalignment of the system sensors (including the model star trackers), however it is important to get an estimate of how well the system performs before declaring success.

In order to calibrate the sensor, the table must be shifted a small (within the FOV of the sensors) amount, and the resulting readings of the sensor compared to the “true” or known table movement.

In many space applications, companies use Theodolites to accurately determine the placement and alignment of components.<sup>5</sup> In keeping with this philosophy a digital theodolite (see Figure 37) was mounted on the testbed to record “true” testbed motion in order to correct for misalignment of the star tracker modeler.

---

<sup>3</sup> "Composite Estimate of Spacecraft Sensor Alignment Calibrations", p. 373.

<sup>4</sup> Composite Estimate of Spacecraft Sensor Alignment Calibrations", p. 371.

<sup>5</sup> Discussion with Dr. Nelson Pedreiro, Lockheed Martin Corporation.



Figure 37. The Nikon NE-20S Digital Theodolite

Two points were marked in the “inertial” reference frame identified in Chapter VI. For this procedure, all differences in measurement (between the theodolite and the star tracker model) were attributed to the star tracker model. This may not be exactly correct, however it will provide a “worst case misalignment” that will be accepted as accurate for the purpose of calibrating the star tracker model.

These points were used as stars for the theodolite. Azimuth and Elevation readings were taken to each “star” at each movement. Similarly, PSM readings were taken at each movement. In total 44 sets of data were collected (see Appendix K). These readings were converted to Euler angles with the convention of X ( $\psi$ ), Y( $\Theta$ ) and Z( $\Phi$ ). Reference Appendix L for the Matlab coding used in conversion.

Each PSD sensor gives two vector direction measurements at every sample. Similarly, the theodolite provides two direction measurements (azimuth and elevation – thus one vector) to each “star” with every measurement. From the vector directions the deterministic algorithm (Wertz, Spacecraft Attitude Determination and Control, 1978) was used to compute the attitude of the platform. Euler angles were used as attitude parameters.

The difference between theodolite readings and star tracker model readings were analyzed in order to determine what (if any) consistent

misalignment (“systemic error” or bias) existed. An estimation of this bias was then applied to the next set of PSM readings. Since the Theodolite (a Nikon NE-20S) has a precision of  $\pm 10$  arc-seconds ( $48 \mu\text{-rad}$ ) and the star tracker modeler  $\pm 1$  arc-second ( $4.8 \mu\text{-rad}$ ); the sensors were considered calibrated when adjusted sensor readings consistently fell with 22 arc-seconds ( $107 \mu\text{-rad}$ ) of the theodolite readings. The bias matrix was determined to be:

- $\psi +9.5000$
- $\Theta+22.2500$
- $\Phi+12.0250$

The final set of data taken (refer to Appendix K) shows that after applying this correction, the sensors and the theodolite agree to within 22 arc-seconds: our sensors were then considered calibrated.

#### A. ERROR BUDGET

Total system noise (including noise from the sensors, amplifiers, and analog to digital conversion) is minimal. In fact, the noise from all of these components together is so small that it is not distinguishable after quantization occurs. Thus, counting the quantization error (determined to be  $0.61 \mu\text{-rad}$  in Chapter III) as a part of system noise sets the Total system noise error budget to  $0.61 \mu\text{-rad}$ .

Laser wander introduces another component of error into the system. Since the position of the laser beam is only known to within  $3 \mu\text{-rad}$ , an error of that amount must be assumed.

The remaining portion of the error is attributed to misalignment in the mounting of the sensor components and coupling-effects of the motion (tip/tilt/rotation); which were neglected in determining the kinematics equations. These misalignment errors may be reduced using an Alignment Kalman Filter.

The theodolite calibration described above provides an upper-boundary for the total error.

**THIS PAGE INTENTIONALLY LEFT BLANK**

## VIII. CONCLUSIONS

Using diode lasers and photovoltaic sensors, it is possible to model a star tracker capable of providing attitude knowledge to within 4  $\mu$ radians. For laboratories not capable of purchasing an actual star tracker, or laboratories for which a star tracker is not feasible (due to photosensitive equipment or limited views of the sky) this model can be implemented to provide comparable initial attitude information.

### A. SUMMARY

The equipment selected as components make the model a viable and affordable alternative to purchasing a space qualified star tracker. This system functions well, providing precise, accurate readings with few limitations.

#### 1. Resolution

Recall from CH III that our sensor (due to the quantization associated with digital-to-analog conversion) is capable of distinguishing the location of the laser beam spot to 0.002442mm. Using the kinematics equations derived in CH V (calculation using the given geometry after setup) results in a max resolution of  $5.59 \times 10^{-7}$  radians or 0.559 $\mu$ radians. This is approximately the same resolution found in the Lockheed-Martin sensor [11].

#### 2. Precision

The limiting factor in sensor precision is the diode laser. Remember that while the laser was chosen because it was has the most predictable, consistent behavior, some wander still occurs.

The readings taken during the PSD calibration indicated that laser stability (when in SS operation, and after applying a running average filter) averaged 3-4 micro-radians of wander over the sampling time. This is the limiting factor in determining sensor precision; and sets the limit at 4  $\mu$ radians.

### 3. Accuracy

System accuracy is the most difficult of the three to determine; as it involves relating the measured performance to “true”. For this testbed sensor, accuracy has more to do with alignment than it does to precision or resolution.

After the rough correction matrix derived in CH VII it is possible to claim calibration of the sensor at an accuracy within 22 arc-seconds ( $107\mu\text{radians}$ ). It is important to recognize that greater accuracy will be possible during the operation of the spacecraft simulator if a recursive attitude determination approach with sensor misalignment estimation is used. Frequently spacecraft are launched with star trackers having accuracies approaching or exceeding 37 arc-seconds, and are corrected once on orbit (many methods exist, see [17]).

Once the final system is up and running and an Alignment Kalman Filter (AKF) is applied the system accuracy will approach the limitation set by laser accuracy ( $4\mu\text{radians}$ ).

### 4. Limitations

#### a. System Reset

The star tracker modeler requires the testbed to be reset to an initial position at the beginning of each run. For the NPS testbed this is not a critical issue; however it does illustrate that the sensor provides initial (not continuous) attitude knowledge within a narrow field of view.

#### b. Field of View (FOV)

A common trade-off in optics is accuracy vs. field of view. The sensor provides high precision information ( $4\mu\text{radians}$  from a 2-meter-to-wall separation) but the cost is field of view. Examining the kinematic equations derived in Chapter V shows that the 10mm total travel (1/2 of the sensor size) limits the total modeler a FOV (actually an angle of view) of  $0.1365^\circ$ . Another way to say this is that the sensor has a precision of  $4\mu\text{radians}$  and a range of 2383  $\mu\text{radians}$  in any direction. It is possible to increase the angle-of-view by altering the distances used in the sensor construction (the distance between the wall and

the platform, or between the beam splitter and PSM making the largest changes). The angle-of-view can also be increased by using a larger PSD.

## B. RECOMMENDATIONS

I suggest the following recommendations for future work to improve the star tracker model.

### 1. Include a Rough Sensor

The sensor as-is works well as a fine pointing sensor; the primary drawback is the limited FOV. By expanding on the idea proposed in CH2-A a simple coarse sensor could easily be incorporated into the testbed using commercial off the shelf (COTS) camera/CCD technology. Using the equations presented in CH2 to achieve – not the  $10\mu\text{radian}$  system requirement, but a  $0.12^\circ$  capability (after which the star tracker can take over) this arrangement becomes much more plausible. The optics requirement changes from 1-meter to a 0.57 mms.

### 2. Add a Second PSM to Each Sensor

In the initial trials a second PSD was used to ensure that readings on laser movement could not be attributed to sensor error.

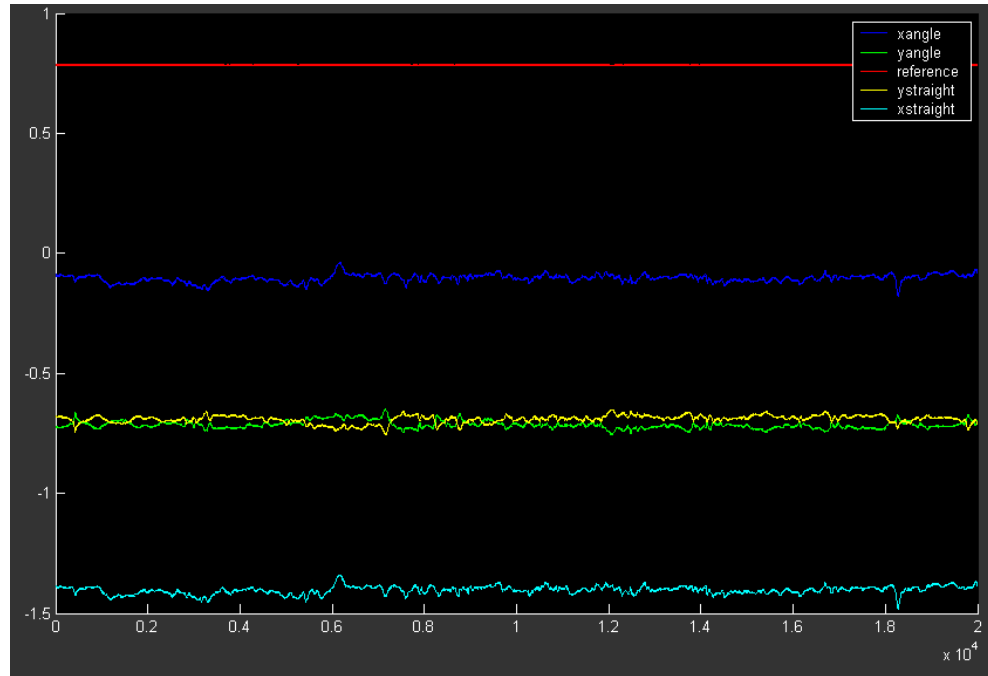


Figure 38. Laser Wander differencing using opposing PSMs

Notice in Figure 38 that because one of the PSMs was mounted upside down, the Y axis readings were inverted. By mounting a second PSD into each of the two sensors, the effects of laser wander could be removed from the system. This could (feasibly) increase the system precision very close to the level of resolution ( $0.559\mu\text{radians}$ ) – nearly an order of magnitude improvement!

### **3. Move Table Closer to Increase FOV**

Another way to deal with the limited FOV is to reduce the distance between the laser and the mirror. The simplest way to achieve this is to move the testbed closer to the walls. If this is done in conjunction with the addition of a PSD to limit beam wander effects, the overall system precision could be improved while dramatically increasing sensor FOV.

### **4. Use a Wavelength Discriminating Filter**

The setup as-is suffers from extreme photosensitivity. Changes to the current lighting configuration are interpreted by the PSD as a shift in laser beam location (since the OT-301 amplifier averages the light readings). By covering the PSM with a wavelength discriminating (bandwidth) filter, the “noise” of overhead lights could be removed from the system. This will entail a re-calibration of the PSMs themselves (as in CH VI); however the overall benefit would merit the effort.

### **5. Perform Testbed Alignment Kalman Filter (AKF)<sup>6</sup>**

As mentioned previously, the correction applied to the alignment is cursory. It is the intention of the testbed engineer to perform an AKF once all on-board sensors are installed and aligned. This method, discussed in greater detail in reference [17] will increase overall sensor accuracy to that commiserate with actual (space qualified) Star Trackers.

---

<sup>6</sup> "Composite Estimate of Spacecraft Sensor Alignment Calibrations", p. 371.

## APPENDIX A – PSM DATASHEETS

**PSM Series**

### Position Sensing Modules

For Non-Contact Measurement Of:  
Position, Motion, Distance And Vibration



**Features**

- Fully Packaged Position Sensing Detectors
- Silicon Linear: 400-1100 nm
- Silicon Duolateral: 400-1100 nm
- Silicon Quadrant: 400-1100 nm
- Germanium Tetra-Lateral: 800-1800 nm
- Removable Filter Holder Adapter
- Standard Mounting Holes
- Plug and Play Compatibility with all ON-TRAK Position Sensing Amplifiers

**ON-TRAK<sup>®</sup>**  
Photonics, Inc.

## PSM Series Position Sensing Modules. Plug-And-Play Precision.

On-Trak Position Sensing Modules are fully packaged position sensing detectors that, when used with an On-Trak position sensing amplifier, provide an analog output directly proportional to the position of a light spot on the detector active area.

Yet, what truly sets them apart is their proprietary, plug-and-play design. Never has position sensing been so convenient... or accurate.

### Finally, A Plug-And-Play Solution.

No more hassling with breadboards, soldering, cutting and wiring. Instead, all On-Trak Position Sensing Modules (PSMs) incorporate a subminiature 9-pin connector that plugs directly into any On-Trak Position Sensing Amplifier.

Just plug it in and go. It's that simple.

1. OT-301 Versatile Position Sensing Amplifier
2. OT-302 Display Module
3. PSM2-10 Position Sensing Module
4. Laptop Computer with BeamTrak software

### Single, Duolateral, Quadrant.

Select from several distinct configurations; each module contains a linear, duolateral, tetralateral, or quadrant position sensing detector. All modules are conveniently packaged to allow simultaneous monitoring of position and light intensity. Position Sensing Modules come in two package sizes: Standard and Compact. The standard measures 2.8" x 2.45" x 1.125". The compact measures 1.25" x 1.25" x 0.975".

### Filters And Filter Holder Adapters.

Harsh ambient lighting conditions? No problem. Each module readily accepts a complete range of optional filters to

reduce the effect of noise caused by ambient light. Moreover, a filter holder is included with each module at no extra cost.

### Standard Mounting Holes.

All PSMs feature standard mounting holes for easy mounting with your existing lab equipment. Whether your post and stands are 1/4 - 20 or 8/32, you'll be up and running in a matter of minutes.

### Robust Aluminum Housings.

On-Trak Position Sensing Modules are encased in rugged aluminum housings to protect your investment.



## PSM Specifications

Model	Active Area (mm)	Detector Type	Wavelength Range	Package Type	Typ. Resolution	Typ. Linearity
PSM 1-2.5	2.5 x 0.6	Linear Silicon	400-1100 nm	Compact	62.5 nm	0.1%
PSM 1-5	5.0 x 1.0	Linear Silicon	400-1100 nm	Compact	125 nm	0.1%
PSM 1-10	10.0 x 2.0	Linear Silicon	400-1100 nm	Standard	250 nm	0.1%
PSM 1-20	20.0 x 3.0	Linear Silicon	400-1100 nm	Standard	500 nm	0.1%
PSM 1-30	30.0 x 4.0	Linear Silicon	400-1100 nm	Standard	750 nm	0.1%
PSM 2-2	2.0 x 2.0	Duolateral Silicon	400-1100 nm	Compact	50 nm	0.3%
PSM 2-4	4.0 x 4.0	Duolateral Silicon	400-1100 nm	Compact	100 nm	0.3%
PSM 2-4Q	4.0 x 4.0	Quadrant Silicon	400-1100 nm	Compact	100 nm	N/A*
PSM 2-5G	5.0 x 5.0	Pincushion Tetralateral Germanium	800-1800 nm	Compact	5 $\mu$ m	—
PSM 2-10	10.0 x 10.0	Duolateral Silicon	400-1100 nm	Standard	250 nm	0.3%
PSM 2-10Q	9.0 x 9.0	Quadrant Silicon	400-1100 nm	Standard	100 nm	N/A*
PSM 2-10G	10.0 x 10.0	Pincushion Tetralateral Germanium	800-1800 nm	Standard	5 $\mu$ m	—
PSM 2-20	20.0 x 20.0	Duolateral Silicon	400-1100 nm	Standard	500 nm	0.3%
PSM 2-45	45.0 x 45.0	Duolateral Silicon	400-1100 nm	Standard	1.25 $\mu$ m	0.3%

\* For nulling applications

## PSM Accessories



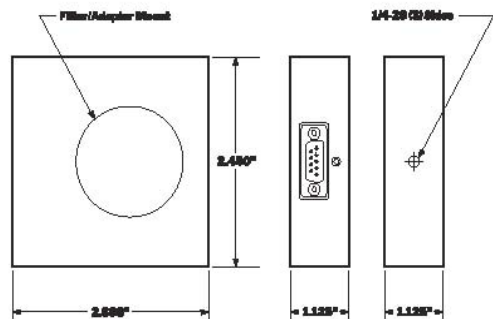
Choose from a wide range of PSM accessories.

Model	Description
<b>F12.5-632.2</b>	12.5 mm optical filter. 632.8 nm, +2.0/-0 nm. FWHM 10 $\pm$ 2 nm. 50% transmittance
<b>F25-632.8</b>	25 mm optical filter. 632.8 nm, +2.0/-0 nm. FWHM 10 $\pm$ 2 nm. 50% transmittance
<b>F12.5-635</b>	12.5 mm optical filter. 635 nm, +5.0/-0 nm. FWHM 10 $\pm$ 2 nm. 50% transmittance
<b>F25-635</b>	25 mm optical filter. 635 nm, +5.0/-0 nm. FWHM 10 $\pm$ 2 nm. 50% transmittance
<b>F12.5-670</b>	12.5 mm optical filter. 670 nm, +3.0/-0 nm. FWHM 10 $\pm$ 2 nm. 50% transmittance
<b>F25-670</b>	25 mm optical filter. 670 nm, +3.0/-0 nm. FWHM 10 $\pm$ 2 nm. 50% transmittance
<b>F12.5-HA</b>	12.5 mm Blank Filter Holder Adapter
<b>F25-HA</b>	25 mm Blank Filter Holder Adapter
<b>CA-DB9MM-5</b>	5 foot molded cable. DB9 connector
<b>CA-SC10FR-3</b>	3 foot ribbon cable. 10 pin socket connector. Unterminated
<b>PS-3</b>	Post and Stand

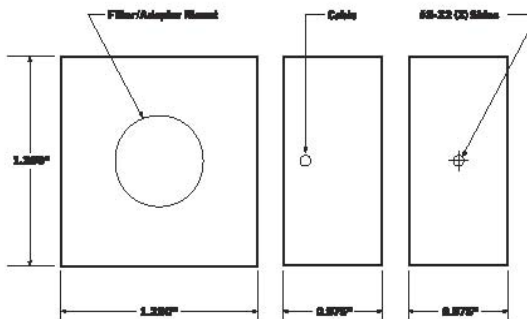
## PSM Series

### Specifications

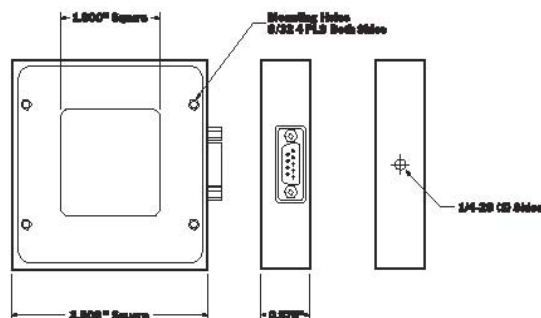
#### Standard Package Drawing



#### Compact Package Drawing



#### PSM2-45



See OT-301 Position Sensing Amplifier brochure for details.



See OT-302D Display Module brochure for details.

**ON-TRAK**  
Photonics, Inc.

26782 Vista Terrace, Lake Forest, CA 92630 Phone: 949-587-0769 Fax: 949-587-9524

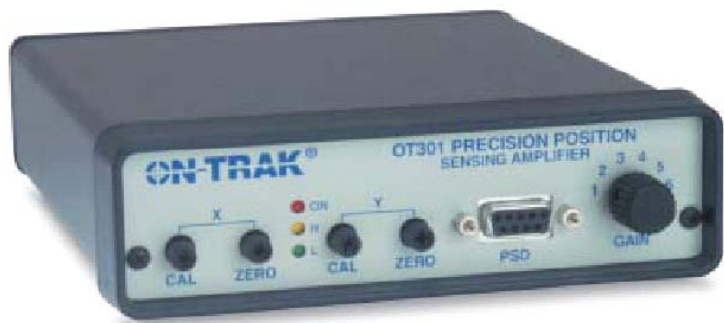
[www.on-trak.com](http://www.on-trak.com)

## APPENDIX B – OT301 AMPLIFIER DATASHEETS

OT-301

### Versatile Position Sensing Amplifier

For: Duolateral • Tetralateral • Quad  
One Dimensional • BiCell



#### Features

- X, Y Analog Position Output Voltages
- Sum Output
- Wide Dynamic Range: 0.1  $\mu$ A to 1.5 mA
- DC to 15kHz
- Compatible With All Position Sensing Detectors
- Zero Offset/Nulling
- Calibration Adjust
- Automatic Detector Bias
- Position Independent of Beam Intensity

**ON-TRAK<sup>®</sup>**  
Photonics, Inc.

## OT-301 Position Sensing Amplifier. Plug-And-Play Convenience And Precision.

The OT-301 Position Sensing Amplifier is the easiest, most precise way to process the current output from any position sensing detector (PSD) on the market.

### Plug-And-Play... Out Of The Box.

Truly plug-and-play, the OT-301 eliminates the hassle of having to design and build a custom amplification solution.

Simply plug in the detector, switch on the power, and you're ready to go.

The benefit is greater convenience, efficiency and productivity... plus 100% compatibility with your future position sensing needs. The OT-301 pays for itself in no time.

### Any Application... Any Detector.

From laser beam alignment, to beam centering, to mirror stabilization, the OT-301 is ideal for one- and two-dimensional absolute optical positioning or precision centering and nulling requirements.

Read the X-Y position output and SUM output from duolateral, tetralateral, single axis, quadrant and bi-cell PSDs.

### X,Y Analog Output That's Directly Proportional To Beam Position.

The photocurrent generated from the position sensing detector is processed by the four-channel amplifier system using a position sensing algorithm. The result is X and Y analog outputs that are directly proportional to beam position—Independent of changes in beam intensity.

### Six Gain Settings: 0.1 $\mu$ A to 1.5 mA.

Six gain settings accommodate input current ranges from 0.1  $\mu$ A to 1.5 mA with a frequency response to 15 kHz. A convenient ZERO adjust enables you to electronically move the zero to a relative position on the PSD. A CAL adjust allows calibration to absolute position.

### Lifetime Warranty.

So reliable is the OT-301, we back it with a comprehensive lifetime warranty... at no additional charge.

### Universal PSD Compatibility

#### One-Dimensional PSD

Common Anode

Common Cathode

#### Two-Dimensional PSD

Duolateral

Tetralateral Common Anode

Tetralateral Common Cathode

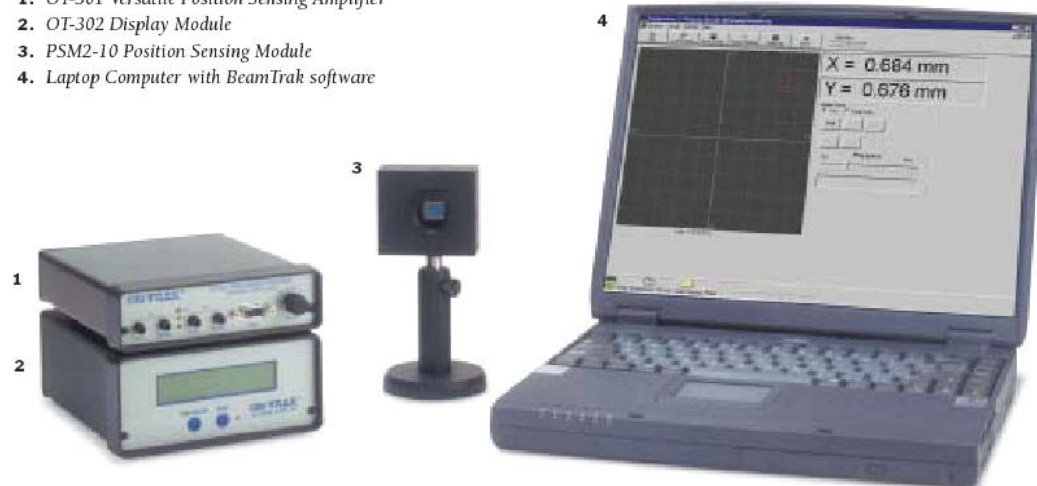
PinCushion Tetralateral-Silicon or Germanium

#### Quad and Bi-Cell

Common Anode

Common Cathode

1. OT-301 Versatile Position Sensing Amplifier
2. OT-302 Display Module
3. PSM2-10 Position Sensing Module
4. Laptop Computer with BeamTrak software



## Front Panel



**Gain:** Transimpedance gain  $4 \times 10^3$  V/A to  $4 \times 10^6$  V/A  
Input current range  $0.1\mu\text{A}$  to  $1.5\text{mA}$ .

**H:** Input optical power exceeds range selected.

**L:** Input optical power lower than range selected. Set range switch at a position where both H/L indicators are off.

**On:** Power on Indicator.

**X,Y Cal:** Gain potentiometers to allow calibration of voltage output in terms of displacement ( $\pm 10\%$  of reading).

**X,Y ZERO:** Enables the user to electronically move the zero to a relative position on the PSD ( $\pm 1\text{V}$  each axis).

**PSD:** DB9 Position Sensing Detector Input.

## Back Panel



**X Out:** Normalized X axis output ( $\pm 10\text{V}$ ).

**Y Out:** Normalized Y axis output ( $\pm 10\text{V}$ ).

**Sum:** Total amplified detector output proportional to light intensity (0-6V).

**CAL/ZERO:** CAL/ZERO "ON" allows use of the X, Y, Zero and X, Y CAL features. CAL/ZERO "OFF" disables these features.

**ON/OFF:** Power ON/OFF.

**Power:** 12V DC 300mA AC adapter.

**THIS PAGE INTENTIONALLY LEFT BLANK**

## APPENDIX C – HENE LASER DATASHEETS



*Product Bulletin*



**Self-Contained Helium-Neon  
Laser Systems  
1500 Series**

The Model 1507 and 1508 Novette™ helium-neon laser systems incorporate hard-sealed internal-mirror 1007 and 1008 plasma tubes and power modules into convenient, compact, self-contained packages. These low-cost units demonstrate superior power stability and meet CDRH requirements.

The base of the Novette is slotted for easy mounting. A 5/8"-32 thread at the beam aperture interface with optical accessories. An optional adapter provides a 1"-32 threaded head (part number 01-0396).

**Key Features**

- Hard-sealed internal mirror plasma tube
- Convenient, compact, self-contained package
- Excellent power stability
- CDRH compliant
- Long operating life

**Applications**

- Alignment
- Metrology
- Inspection

**Compliance**

- CDRH
- UL
- CE

**THIS PAGE INTENTIONALLY LEFT BLANK**

## APPENDIX D – POLARIZED HENE LASER DATASHEET

### 632.8 nm Red Cylindrical Helium Neon Lasers

- 44.5 mm (1.75") diameter long life cylindrical lasers

- 2 - 17 mW TEM<sub>00</sub> power, random or linear polarization

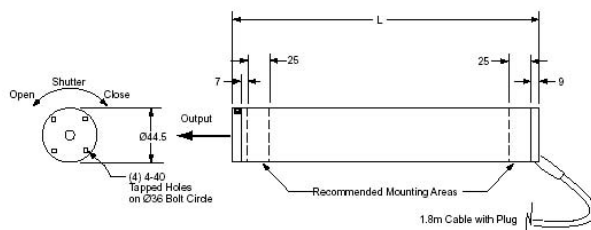


These lasers have been developed with modern intra-cavity optics and construction techniques and assembled in robust larger-diameter (1.75", 44.5 mm) aluminum cylindrical housings for long life stable operation. The lasers are available with either linearly or randomly polarized output beams and models with powers of 2 to 17 mW are available. These powers are minimum values and are warranted for at least one year of operation when the recommended power supplies are used.

These lasers have low-divergence circular (Gaussian) collimated beams with good pointing stability (<0.03 mrad drift after 15 minutes warmup, <0.05 mrad for the 17 mW lasers), less than 1% RMS noise and excellent wavefront quality. The lasers are all TEM<sub>00</sub> with two to four longitudinal modes oscillating (separated by the mode spacing) and the coherence length is typically a few tens of centimeters. For even longer lengths see details of the frequency stabilized HeNe laser on page 24.

#### HeNe Laser Mounts

A wide range of mechanical mounts are available for positioning and aligning cylindrical HeNe lasers. These are summarized on page 30 and more fully described on pages 402-403.



#### 632.8 nm Red Cylindrical Helium Neon Lasers

Catalog Number	Power (mW)	CRDH Class	Wavelength (nm)	Polarization	Beam Size* (mm)	Beam Divergence (mrad)	Mode Spacing (MHz)	Mode Sweep (%)	8-hour Power Drift (%)	Power Supply <sup>†</sup>	Length L (mm)
31-2025	2	IIIa	632.8	>500:1	0.79	1.00	574	<5	<2.5	31-2462	315
31-2033	2	IIIa	632.8	Random	0.79	1.00	574	<5	<2.5	31-2462	315
31-2041	4	IIIb	632.8	>500:1	0.80	1.00	438	<2	<5	31-2405	396
31-2058	4	IIIb	632.8	Random	0.80	1.00	438	<2	<5	31-2405	396
31-2066	7	IIIb	632.8	>500:1	1.02	0.79	373	<2	<2.5	31-2454	456
31-2074	7	IIIb	632.8	Random	1.02	0.79	373	<2	<2.5	31-2454	456
31-2082	10	IIIb	632.8	>500:1	0.65	1.24	341	<2	<5	31-2439	484
31-2090	10	IIIb	632.8	Random	0.65	1.24	341	<2	<5	31-2439	484
31-2108	17	IIIb	632.8	>500:1	0.95	0.84	257	<10	<5	31-2447	637
31-2196	17	IIIb	632.8	Random	0.95	0.84	257	<10	<5	31-2447	637

\* 1/e<sup>2</sup> intensity diameter at laser face. <sup>†</sup> The power supplies are sold separately and are fully described on page 28

US: (800) 343-4912 • UK: 0800 515801 • Germany: +49 6071 968 302 • France: +33 1 60 19 40 40 • Japan: +81 3 5635 8680 **COHERENT**

Diod & Diode Lasers	Light Sources
HeNe Lasers	

Power & Laser Diagnostics	Light Analysis
Laser Optics	

Optics	Apertures, Windows, Filters
Lenses & Beam Splitters	

Opto-Mechanics	Mounting Plates, Mounting Arms, Micro Motors
Breadboards, Mounting Arms	

## HeNe Laser Power Supplies



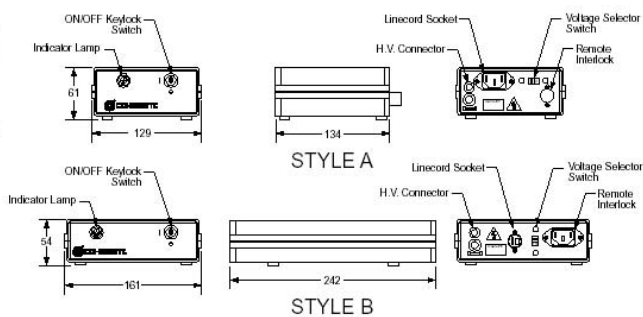
- Range of supplies matched to individual laser heads
- High voltage compliant low-noise constant current sources
- CE certified with all necessary CDRH safety features



The active medium in HeNe lasers is a low pressure mixture of helium and neon. The power supply needs to generate a high voltage pulse (typically 8 to 16 kV) to initiate an electrical discharge in the gas mixture and a voltage (typically 1 to 3 kV) to sustain a controlled discharge of a few millamps. These power supplies have been developed to provide the initial pulse and then act as a current source, automatically adjusting the voltage to maintain the design current. It is crucial to use the correct power supply for each laser, only then will the power supply be correctly compliant to match the combination of the discharge and ballast resistors in the laser head.

These power supplies incorporate all the necessary CDRH safety features, proper insulation for the high voltage circuitry

and output socket, and built-in bleed circuits to prevent charge retention after the laser is switched off.



### HeNe Laser Power Supplies

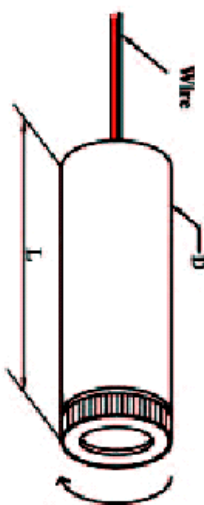
Catalog Number	Compatible Lasers	Style Class	Sustaining Current (mA $\pm 0.2$ mA)	Starting Voltage (kVDC)	Sustaining Voltage (VDC)
31-2405	31-2207 31-2041 31-2058	A	6.5	>10	1850 - 2450
31-2413	31-2230 31-2298	A	6.5	>10	2450 - 2850
31-2421	31-2264	A	5.0	>10	1700 - 2100
31-2439	31-2772 31-2298 31-2082 31-2090	B	6.5	>11	2500 - 4100
31-2447	31-2108 31-2196	B	7.0	>11	2500 - 4100
31-2454	31-2066 31-2074	A	7.0	>10	2450 - 2850
31-2462	31-2025 31-2033	A	6.5	>10	1700 - 2100
31-2470	31-2009 31-2017	A	4.0	>8	1100 - 1500
31-2488	31-2140 31-2157	B	8.0	>16	4400 - 5300

### Electrical, Mechanical and Environmental Specifications

**Temperatures** -  
Operating: -20 to +40 °C  
Non-operating: -40 to +80 °C  
**Input Power**: 115/230 VAC 50 - 400 Hz, rear panel switch  
IEC socket for detachable cord (1.8 m cord supplied)  
**Power Consumption** -  
Style A: ~ 25 W  
Style B: 30 - 50 W  
**Laser Safety**: Keyswitch (3 - 7 s delay), on/off indicator and safety interlock  
Manual shutter on lasers  
**Certification**: CE  
**Dimensions**: See drawings  
**Weights** -  
Style A: 1.1 kg  
Style B: 1.5 kg

## APPENDIX E – DIODE LASER DATASHEETS

### Laser Diode Module Part No : UL5-1G-635



OPTICAL	
Wavelength	635
Optical Output Power	1 mW
Stability	<1 %
Laser Class	Class II
Laser Operation	Continuous
Laser Structure	Single Mode Laser
Divergence at the collimation	<0.5 milliradian
Spot Size	Adjustable
Minimum Spot Size	< 1 mm up to 10 ft
Bore sight Accuracy	2.5 milliradian

#### Product Features

- Hard Anodized Aircraft Aluminum Body
- Auto-Power Control Circuitry for high stability
- Elliptical spot laser for high efficiency and clean beam
- Collimated or Adjustable focus beam
- High Degree of Optico-Mechanical Alignment
- Custom Options Available

#### ELECTRICAL

Operating Voltage	3 to 5 VDC
Operating Current	<60 mA
Auto Power Circuit	Yes
Electrical Connections	+Red, -Black

#### MECHANICAL

Dimensions (L x D), mm	26 mm L x 10.5 mm D
Operating Temperature	-10°C to +55°C
Storage Temperature	-40°C to +80°C
Heat Sink Requirements	Recommended for extended use

#### Operational Hazard-Semiconductor Laser Diode Module

This laser module emits radiation that is visible and harmful to human eye. When in use, do not look directly into the laser emitting aperture. Direct viewing of laser diode emission at close range may cause eye damage, especially in conjunction with the collimating lenses. Extreme care must be taken to prevent the beam from being viewed directly or through external optics or mirrors.

**World Star Tech.**  
321 Lamellar Rd. Toronto, Ont. M3B 2R1 Canada  
Tel: (416) 365-3332 Fax: (416) 365-3112 [www.worldstartech.com](http://www.worldstartech.com)

**Limited Warranty:** World Star Technologies warrants to the original purchaser, that the product will be free of manufacturing defects in materials and workmanship for a period of 12 months after the product delivery. No warranty coverage for dimension, modifications or damage due to abuse or misapplication.

**THIS PAGE INTENTIONALLY LEFT BLANK**

## APPENDIX F – AEROTECH NANO-POSITIONER DATASHEETS

### MANUAL NANO-POSITIONERS |

- Linear resolution is 25 nm
- Linear digital readout resolution is 10 nm
- Rotary resolution is 0.1 arc-second
- Decoupled orthogonal movement
- 360° rotation
- Cross-roller bearings
- Low profile
- Excellent thermal stability



ATT185-3



ATT185-5



ARS301

In those cases where a completely automated system is not required, or where one or more axes needs very infrequent adjustment, or perhaps in early stage proof-of-concept laboratory experiments, Aerotech's manual stages can do the job. Aerotech offers a line of nanometer resolution, large travel range, rotary and linear tables. These manual stages, which have been used extensively by the major research laboratories throughout the world over the past thirty years, offer excellent in-position stability, high positioning resolution, large adjustment range, and outstanding thermal stability.



WORLD HEADQUARTERS: Aerotech, Inc., 101 Zeta Drive, Pittsburgh, PA 15238, USA 412-963-7470 Fax: 412-963-7459  
Aerotech, Ltd., Jupiter House, Calleva Park, Aldermaston, Berkshire RG7 8NN, UK 44-118-9409400 Fax: 44-118-9815022  
Aerotech GmbH, Südwestpark 90, 90449 Nürnberg, Germany +49-911-9679370 Fax: +49-911-96793720

[www.aerotech.com](http://www.aerotech.com) 

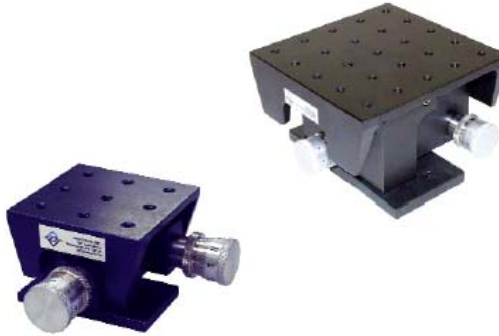
## PRECISION TILT TABLES

- Sub-arc-second resolution
- Decoupled, orthogonal tilting movement
- High thermal stability

The ATT185 series precision tilt (pitch-roll) tables provide a means for leveling instruments or tilting components over a  $\pm 10^\circ$  range. Aerotech's patented\* sub-arc-second resolution drive allows the user to cover the total angular range quickly while maintaining a resolution of 0.2 arc-second for the ATT185-3, and 0.1 arc-second for the ATT185-5. With this unique drive, the tables exhibit virtually no creep or backlash and have excellent repeatability. These tables have a gimbal support with decoupled and orthogonal axial motion.

Both tilt table bases have clearance holes for M6 screws on 25 mm centers and are adaptable to Aerotech linear or rotary translation stages. The tables are constructed of aluminum with a black anodized finish.

\*U.S. Patent #3,727,471



	ATT185-3	ATT185-5
Range	$\pm 10^\circ$	
Thimble Graduation	5.0 arc-second	2.5 arc-second
Resolution*	0.2 arc-second	0.1 arc-second
Max Load (Horizontal)**	4.54 kg (10 lb)	
Material	Aluminum	
Finish	Black Anodized	
Weight	0.5 kg (1.1 lb)	1.41 kg (3.1 lb)

\*per 0.5° movement of the fine adjustment.

\*\*Load should be centered or counterbalanced to provide accurate tilt.



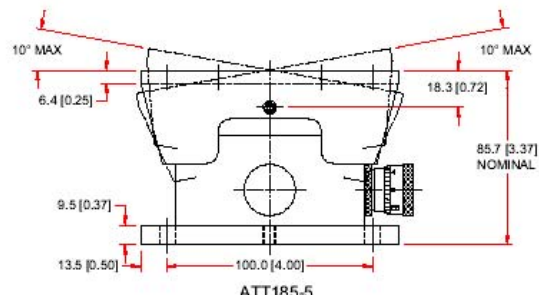
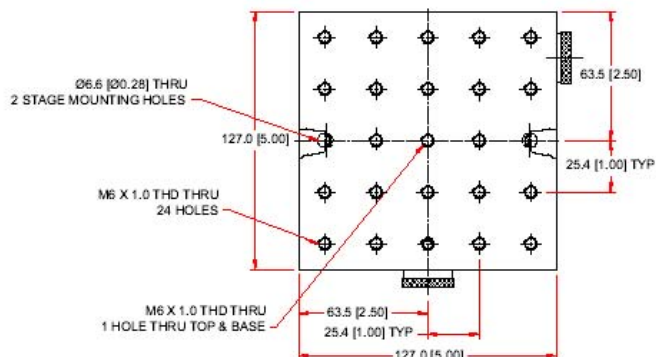
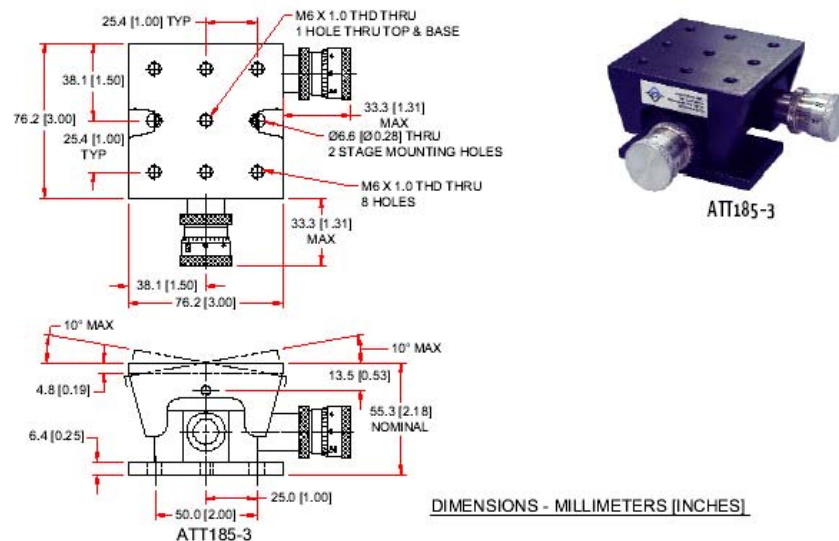
[www.aerotech.com](http://www.aerotech.com)

WORLD HEADQUARTERS: Aerotech, Inc., 101 Zeta Drive, Pittsburgh, PA 15238, USA 412-963-7470 Fax:412-963-7459  
Aerotech, Ltd., Jupiter House, Calleva Park, Aldermaston, Berkshire RG7 8NB, UK 44-118-9409400 Fax:44-118-9815022  
Aerotech GmbH, Südwestpark 90, 90449 Nürnberg, Germany +49-911-9679370 Fax:+49-911-96793720



## ATT185-3 and -5 DIMENSIONS |

Dedicated to the Science of Motion



WORLD HEADQUARTERS: Aerotech, Inc., 101 Zeta Drive, Pittsburgh, PA 15238, USA 412-963-7470 Fax: 412-963-7459  
 Aerotech, Ltd., Jupiter House, Calleva Park, Aldermaston, Berkshire RG7 4NN, UK 44-118-9409400 Fax: 44-118-9815022  
 Aerotech GmbH, Südwestpark 90, 90449 Nürnberg, Germany +49-911-9679370 Fax: +49-911-96793720

[www.aerotech.com](http://www.aerotech.com)



## MANUAL ROTARY POSITIONING STAGE

- 360° rotation
- Excellent thermal stability
- Patented sub-arc-second resolution drive

The ARS301 stage is a precise rotary positioner featuring Aerotech's patented sub-arc-second resolution drive mechanism. By depressing the release plunger, the rotary ring of the ARS301 can be quickly positioned to the approximate desired angle. It can then be fine-tuned with either the coarse or fine adjustment knob over a range of 10 degrees or 30 minutes, respectively. This stage achieves a 0.1 arc-second resolution. The fine thimble has a 32-division reference scale for convenience in positioning. An engraved dial with a six-minute vernier is standard on all tabletops. Due to the absence of any gearing in the ARS301's drive mechanism, the stage is backlash free.

The ARS301 has a 68 mm (2.68 in) clear aperture. If a solid mounting surface is required, the ARS301TT is available. The ARS301TT has a grid of M6 mounting holes on 25 mm centers. The ARS301 is made of aluminum with a black anodized finish and weighs 1.36 kg (3 lb).



ARS301

### ARS301

Thimble Graduation	2.54 arc-second
Resolution*	0.1 arc-second
Max Load (Horizontal)	11.36 kg (25 lb)
(Vertical)	6.82 kg (15 lb)
360° Dial and 6 Minute Vernier	Standard
Clear Aperture	68.07 mm (2.68 in)

\*Per 0.5° movement of the fine adjustment.



[www.aerotech.com](http://www.aerotech.com)

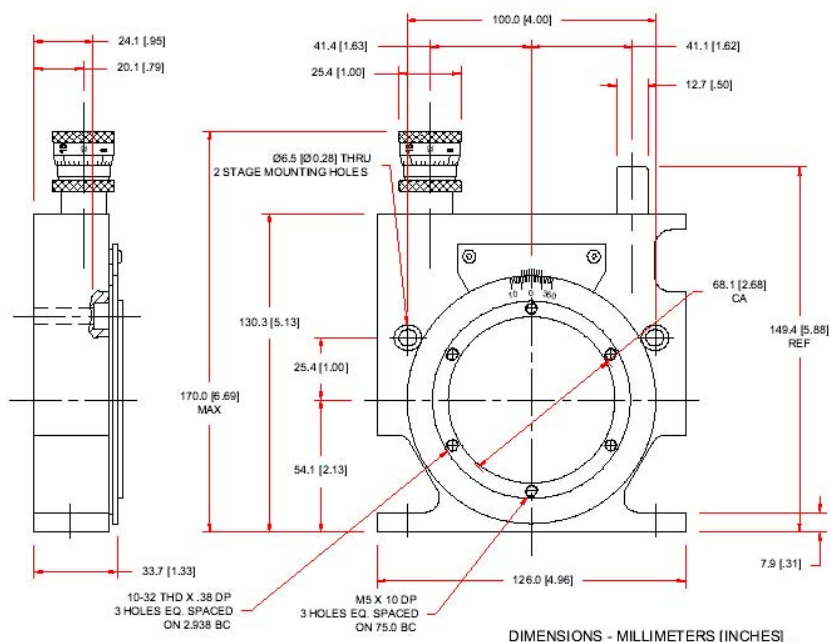
WORLD HEADQUARTERS: Aerotech, Inc., 101 Zeta Drive, Pittsburgh, PA 15238, USA 412-963-7470 Fax: 412-963-7459  
Aerotech, Ltd., Jupiter House, Calleva Park, Aldermaston, Berkshire RG7 8NN, UK 44-118-9409400 Fax: 44-118-9815022  
Aerotech GmbH, Südwestpark 90, 90449 Nürnberg, Germany +49-911-9679370 Fax: +49-911-96793720



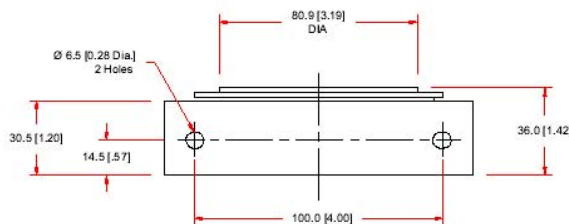
## ARS301 DIMENSIONS |

*Dedicated to the Science of Motion*

ARS301



DIMENSIONS - MILLIMETERS (INCHES)



WORLD HEADQUARTERS: Aerotech, Inc., 101 Zeta Drive, Pittsburgh, PA 15238, USA 412-963-7479 Fax: 412-963-7459  
 Aerotech, Ltd., Jupiter House, Colleva Park, Aldermaston, Berkshire RG7 8NN, UK 44-118-9409400 Fax: 44-118-9815022  
 Aerotech GmbH, Südstaempfplatz 90, 90449 Nürnberg, Germany +49-911-9679370 Fax: +49-911-96793720

[www.aerotech.com](http://www.aerotech.com)

**THIS PAGE INTENTIONALLY LEFT BLANK**

## APPENDIX G – LASERMARK® MP5 FIVE-BEAM LASER

**LASERMARK®**



**MP5 Five Beam Laser**

**Plumb, Level, and Square instantly up to 100 feet!**

The MP5 Self-Leveling Laser is 21st century's "must have" productivity and accuracy enhancing tool. Five independent self-leveling 650nm highly focused laser beams provide accuracy of 1/4-inch at 100 feet. Turn it on and go to work, no bubbles; and it levels itself to  $\pm 5^\circ$ . Gravity design pendulum self-levels instantly and automatically with a unique magnetic dampening system.



**Low Power Indicator:** Laser blinks 4 times every eight seconds

**Out of Level Indicator:** Laser blinks rapidly

**Use for:** Leveling, Squaring, and Plumbing-Decks/Porches/Foundations, Transferring Points from Floor to Ceiling, Finish Carpentry, HVAC, Plumbing, Pipe Installation, Plumbing and Aligning Walls, Doors and Skylights, Installing Trim and Mill Work, Leveling Electrical Outlets, Determining Grade

---

### SPECIFICATIONS

**Laser Diode** 650nm Visible Red Beam, class IIIa

**Leveling Accuracy** 1/4" at 100' (6mm at 30m)

**Visibility Range** up to 100' (30m)

**Weight** 1lb 3.2 oz. (545g) with Batteries

**Power** Three (3) "AA" batteries (4.5VDC)

**Indicating Lights** Low Power: Laser blinks four times every eight seconds  
Out of Level: Laser blinks rapidly

**Universal Base** 7.1 oz. (202g)

**Includes** laser, multi-mount accessory, mounting strap, target, padded carrying case, batteries and manual

**Warranty** One Year

---

### CST ITEMS

58-MP5

Five Beam Laser Includes: Multi-Mount, Laser Trivet, Target, Strap, Carrying Case, and Manual

**THIS PAGE INTENTIONALLY LEFT BLANK**

## APPENDIX H – MAGNETIC POLYCAST® PROTRACTOR



### EMPIRE LEVEL MFG. CORP.

- 929 Empire Drive
- Mukwonago, WI 53149
- Phone: 1-262-368-2000
- Customer Service Phone: 1-800-558-0722
- Fax: 1-262-368-2131
- Email: [empire@empirelevel.com](mailto:empire@empirelevel.com)
- Web: <http://www.empirelevel.com/>



©2003 Empire Level Mfg. Corp.  
All rights reserved.

### Magnetic POLYCAST® Protractor



- Transfer angles to within 1 degree
- Magnetic base and back
- Built-in pitch calculator on back

# 36

**THIS PAGE INTENTIONALLY LEFT BLANK**

## APPENDIX I – KINEMATIC MIRROR MOUNTS

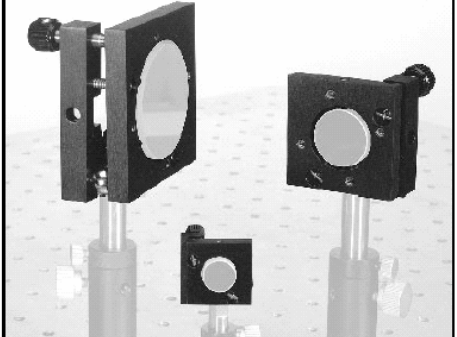
Lens Filter & Polarizer Mounts

Mirror/Beamsplitter Mounts & Prism Tables

Posts, Pillars, Bases & Adaptor Plates

Rail & StableRod<sup>™</sup> Mounting Systems

Microscope Components, Spatial Filters & Apertures



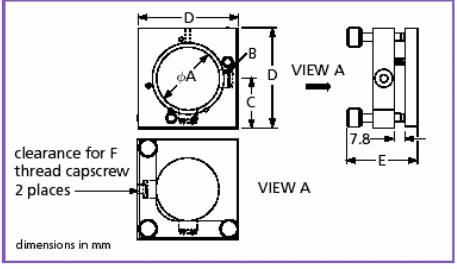
Available in:  
 ✓ Production Quantities  
 ✓ Custom Sizes

### Kinematic Mirror/Beamsplitter Mounts

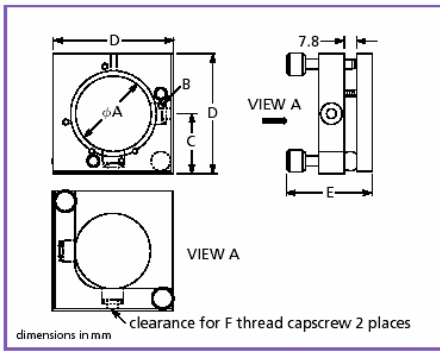
Kinematic mirror/beamsplitter mounts are an ideal low-cost solution for tilt in two axis. The kinematic design incorporates hardened surfaces to resist wear and increase stability.

- Precision stainless-steel adjustment screws with brass threaded inserts provide exceptionally smooth adjustment.
- Triple-adjustment mounts provide translation and tilt.
- Counter-bored holes provided for easy attachment to mounting posts. See Chapter 26, *Posts, Pillars, Bases and Adaptor Plates*.
- The mounts have an angular range of 10 degrees.
- M6 and 1/4-20 or M4 and 8-32 cap screws are provided.

**07 MHT 03X kinematic mounts with three adjusters**



**07 MHT 02X kinematic mount with two adjusters**



**07 MHT Kinematic Mirror/Beamsplitter Mounts**

Optic Diameter	Angular* Resolution	Number of Adjusters	B Hole Pattern	Optical Axis Height				PRODUCT NUMBER
$\phi A$	Arc sec	2	M2 on 20 mm center	C (mm)	D (mm)	E (mm)	F (mm)	
16	20 arc sec	2	M2 on 20 mm center	15	27.5	28	M4 or 8-32	07 MHT 021
12.5-12.7	20 arc sec	2	M2 on 20 mm center	15	27.5	28	M4 or 8-32	07 MHT 023
25.0-25.4	10 arc sec	2	M4 on 38 mm bolt circle	25	50	50	M6 or 1/4-20	07 MHT 025
50.0-50.8	6 arc sec	2	M4 on 60 mm bolt circle	37.5	75	53	M6 or 1/4-20	07 MHT 027
16	20 arc sec	3	M2 on 20 mm center	15	27.5	28	M4 or 8-32	07 MHT 031
12.5-12.7	20 arc sec	3	M2 on 20 mm center	15	27.5	28	M4 or 8-32	07 MHT 033
25.0-25.4	10 arc sec	3	M4 on 38 mm bolt circle	25	50	50	M6 or 1/4-20	07 MHT 035
50.0-50.8	6 arc sec	3	M4 on 60 mm bolt circle	37.5	75	53	M6 or 1/4-20	07 MHT 037

\*Angular resolution calculated from 2° rotation of adjuster.

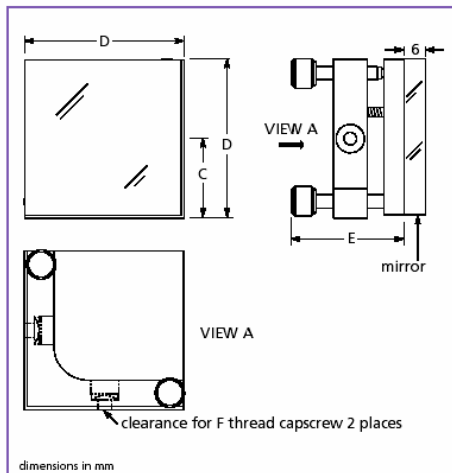
25.2 **MELLES GRIOT**

Visit Us OnLine! [www.mellesgriot.com](http://www.mellesgriot.com)

**KINEMATIC MOUNTS WITH MIRROR**

Our kinematic mounts are available with a ready-to-go mounted mirror.

- Premounted λ/4 flat mirror
- /001 MAXBRite™ coating for 480–700 nm

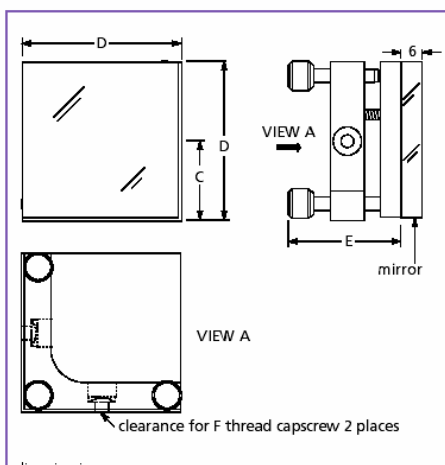


07 MHT 024 / 07 MHT 026

**07 MHT Kinematic Mounts with Mirror**

Mirror Size			Optical Axis Height			PRODUCT NUMBER
D (mm)	Angular* Resolution	Number of Adjusters	C (mm)	E (mm)	F	
25×25	20 arc sec	2	15	35	M4 or 8-32	07 MHT 024
	20 arc sec	3	15	35	M4 or 8-32	07 MHT 034
50×50	10 arc sec	2	25	54	M6 or 1/4-20	07 MHT 026
	10 arc sec	3	25	54	M6 or 1/4-20	07 MHT 036

\*Angular resolution is calculated from a 2° rotation of adjusting screw.



07 MHT 034 / 07 MHT 036

Visit Us Online! [www.mellesgriot.com](http://www.mellesgriot.com)

**MELLES GRIOT** 25.3

## APPENDIX J– KINEMATIC BEAM SPLITTER MOUNTS

(used for mounting the pellicle beam splitters)

### Series 260 Mirror Mounts

CVI Laser, LLC  
800-296-9541

Series 260 Mirror Mounts are perfectly sized for demanding breadboard and instrumentation applications using larger optics. Six models hold mirrors from 1.50" to 3.00". Both English and Metric taps and bores available. Model 260-30 is the most compact, cost-effective precision 3.00" mirror mount available.

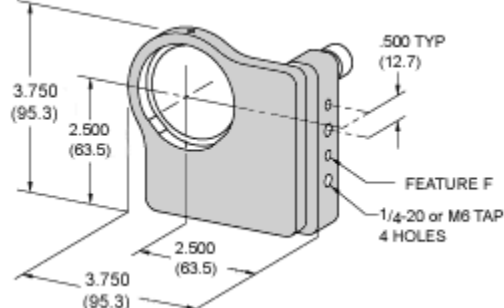
Rugged construction features a .75" thick support frame and hardened bearing points. The large 2.63" moment arms provide a tilt range of  $\pm 4.8^\circ$  and a sensitivity of  $13\mu\text{rad}/^\circ$ . The 3SC models permit translation and focusing of the mirrors over a range of  $\pm 5.5\text{mm}$  ( $\pm .22"$ ). The 3SC models permit translation and focusing of the mirrors over a range of  $\pm 5.5\text{mm}$  ( $\pm .22"$ ).

#### Lockable Nuts

All of our full size mirror mounts are now available with locking nuts

#### 260-B1 Base

The beam height of this series can be raised to 3.00" above the mounting surface when base 260-B1 is used. It also gives you more flexibility in mounting with 1/4-20 (M-6) slot.



**THIS PAGE INTENTIONALLY LEFT BLANK**

## APPENDIX K – CALIBRATION DATA

X Elevation – Elevation as measured from the Theodolite to Star X

X Azimuth – Azimuth as measured from the Theodolite to Star X

Z Elevation – Elevation as measured from the Theodolite to Star Z

Z Azimuth – Azimuth as measured from the Theodolite to Star Z

Z PSD X – The “X” reading off the PSD mounted on the Z axis

Z PSD Y – The “Y” reading off the PSD mounted on the Z axis

X PSD Y – The “Y” reading off the PSD mounted on the Z axis

X PSD X – The “X” reading off the PSD mounted on the Z axis

X Elevation	X Azimuth	Z Elevation	Z Azimuth	Z PSD X	Z PSD Y	X PSD Y*	X PSD X*
90 00 00	00 00 00	90 00 00	270 00 00	0.00171916971917	-0.00517216117216	0.00255921855922	-0.0005616605616
90 01 00	1 40	90 00 20	270 02 00	2.38667155067154	0.45755799755800	-1.06735042735043	-2.08861050061051
90 01 20	359 56 00	90 02 00	269 55 40	-5.47578998779004	2.35557020757021	-1.25468131868131	5.04706227106231
90 02 40	7 40	89 53 40	270 08 00	9.17380708180710	-7.53964346764358	-3.47590720390720	-9.07657142857139
90 02 20	5 40	90 00 00	270 06 40	8.16855677655693	-0.03232722832723	-2.49115506715507	-7.39403663003651
89 55 40	359 53 00	90 03 20	269 52 20	-9.50168498168497	4.05798778998783	5.80629059829063	8.78975824175831
90 00 00	359 57 40	89 54 00	269 57 00	-4.10096214896210	-7.36869841269848	-0.14419536019536	3.42681807081811
89 55 00	3 40	89 53 00	270 03 40	4.19444688644685	-8.78325274725277	6.17943345543352	-4.24272527472530
90 03 4	3 20	89 53 00	270 03 20	3.59934554334551	-8.79936507936514	-4.65614163614166	-3.7092046520151
89 54 00	359 59 00	89 53 20	269 58 20	-2.33612210012212	-8.49957977557997	7.27677167277156	1.85415384615385
89 57 00	359 59 20	90 06 20	269 59 40	-0.10036141636142	7.77909157509150	4.72268620268620	0.35964835164835
90 05 40	40	90 04 20	270 01 00	1.45243956043956	5.37209768009769	-6.17462759462764	-1.24690109890110
89 53 20	359 59 20	90 05 00	269 59 40	-0.13365079365080	5.94973870573862	8.75329914529911	0.40293040293040
89 53 00	359 53 40	90 06 20	269 53 20	-8.09055921855919	7.41665934065943	8.80015628815634	7.67712820512829
90 06 40	359 53 00	90 04 00	269 52 40	-9.32341391941394	5.55941391941395	-7.28764835164843	8.42200732600744
90 05 20	7 20	89 53 20	270 07 40	8.95057387057383	-7.62258363858366	-6.44779975579973	-8.93879853479857
90 05 40	359 55 00	89 52 40	269 54 00	-8.18466422466425	-8.76094749694739	-6.99433455433458	7.00085470085471
90 04 00	359 56 00	90 01 20	269 55 40	-5.38204639804634	2.13216117216116	-4.33476923076924	4.84259340659337
90 05 00	7 00	89 59 40	270 08 00	9.88440048840038	-0.78043956043956	-5.69519902319896	-9.04533821733825
89 57 40	359 57 00	89 59 40	269 56 20	-4.50884493284488	-0.69723565323564	3.5958536385835	4.09952625152623
89 57 00	3 40	89 54 40	270 03 40	4.52535286935289	-7.05354334554342	4.08655921855922	-4.33871550671551
89 54 20	359 55 40	89 57 00	269 54 40	-6.58689621489613	-4.01321611721612	7.41689377289388	5.90778998779003
89 55 20	3 00	89 54 40	270 02 40	3.48012210012208	-6.91147741147748	5.92615873015879	-3.38683272283269
89 58 00	40	89 59 20	270 00 40	0.80141147741148	-1.05120390720390	2.87571184371185	-0.79458852258852
89 54 00	1 20	89 57 40	270 01 20	1.77903785103786	-3.25256654456653	8.12988522588521	-1.69347008547008
89 58 40	359 58 20	89 58 00	269 57 40	-2.60391697191696	-2.39390476190478	1.94839072039072	2.08235409035409
89 59 20	359 59 00	90 02 40	269 59 00	-0.92299389499389	3.279003663300369	1.65415873015872	0.68129914529914
89 59 40	359 59 00	89 54 00	269 58 20	-2.34973870573871	-7.57486691086680	0.89270329670329	1.47700610500611
90 05 00	359 55 40	89 56 00	269 54 40	-6.82474236874229	-4.71872527472523	-5.71890598290600	5.89860805860801
89 55 20	3 20	89 54 40	270 03 00	3.95539926739934	-7.12527960927960	6.15011477411475	-3.83329914529916
90 00 40	3 40	90 04 20	270 04 20	5.92036630036642	5.29738217338221	0.36401465201465	-5.25641025641021
90 05 40	4 00	90 03 40	270 05 00	6.33988278388270	4.36873260073265	-5.99984371184373	-5.70974847374841
90 00 20	6 20	89 56 20	270 06 20	8.13838827838814	-4.98518192918195	0.00995360195360	-7.54800976800986
90 01 40	359 53 40	89 58 40	269 53 00	-8.87142857142860	-1.17248351648352	-1.31805128205128	7.94437606837601

90 01 40	5 20	90 00 00	270 05 40	7.48769230769243	-0.10303785103785	-1.40631990231990	-6.82520146520142
90 03 20	359 53 00	89 59 20	269 52 20	-9.91246398046402	-0.41707448107448	-3.58425396825397	8.79164346764351
89 56 40	7 00	89 54 20	270 07 20	8.98079120879134	-7.50206593406591	4.337557997555800	-8.50001953601954
89 57 40	0	89 59 20	270 00 00	0.05861782661783	-0.91582905982906	3.63448107448107	-0.2051280512821
89 58 20	359 56 00	89 53 00	269 55 00	-6.62703785103783	-8.36118681318694	1.94843956043956	5.66532844932850
90 02 40	359 57 00	89 55 00	269 56 00	-5.17176068376075	-6.06873748473743	-2.98855677655678	4.38338949938947
90 05 20	359 58 20	90 04 40	269 58 20	-1.91789499389500	5.93951648351647	-5.44346275946271	1.80041514041514
89 54 00	359 59 40	90 00 00	269 59 20	-0.47084737484738	-0.31789499389499	8.30108913308920	0.36822954822955
90 02 40	0	89 54 40	269 59 20	-0.87414896214896	-6.34427838827839	-2.90584126984127	0.48925030525030
90 01 00	359 58 20	89 57 00	269 57 40	-2.78238339438337	-3.37038339438342	-0.96086935286935	2.31764102564102

Euler_angles_deg_theod	Euler_angles_deg	Difference (seconds)	sectional averages	Adjusted averages after applying overall correction
0 0 0	0 0 0	0		
0 0 0	0 0 0	0		
0 0 0	0 0 0	0		
0 0 21	0 0 17	4		
0 -1 -2	0 0 -44	-18		
0 1 55	0 1 26	29		
0 1 59	0 1 39	20		
0 -1 -18	0 0 -52	-26		
0 -4 -14	0 -3 -44	-30		
0 -6 -4	0 -5 -14	-50		
0 -3 -18	0 -2 -25	-53		
0 7 42	0 6 58	44		
0 0 4	0 0 -5	9		
0 -2 -29	0 -1 -44	-45		
0 6 26	0 5 14	72		
0 3 6	0 2 54	12		
0 4 53	0 3 33	80		
0 -7 -21	0 -6 -31	-50		
0 -5 -49	0 -5 -2	-47		
0 0 -27	0 0 -6	-21		
0 -2 -55	0 -1 -53	-62		
0 -6 -57	0 -6 -1	-56		
0 4 53	0 4 19	34		
0 3 41	0 3 38	3		
0 -6 -41	0 -6 -6	-35		
0 -4 -28	0 -3 -15	-73		
0 3 8	0 3 16	-8		
0 -6 -39	0 -5 -47	-52		
0 5 58	0 5 5	53		
0 -1 -28	0 0 -41	-47		
0 6 3	0 5 24	39		
0 3 42	0 3 17	25		
0 0 -15	0 0 -49	34		
0 4 23	0 3 39	44		
0 -5 -47	0 -4 -19	-88		
0 0 51	0 0 29	22		
0 4 38	0 4 10	28		
0 7 34	0 6 6	88		
0 0 -10	0 0 -43	33		
0 5 56	0 5 14	42		
0 8 0	0 6 8	112		
0 -6 -19	0 -5 -59	-20		
0 4 6	0 3 51	15		
0 -6 -56	0 -5 -5	-111		
0 -7 -16	0 -6 -21	-55		
0 -6 -18	0 -5 -19	-59		
0 -6 -13	0 -4 -30	-103		
0 7 19	0 6 53	26		
0 -6 -56	0 -6 -1	-55		
0 -6 -41	0 -4 -53	-96		
0 -5 -59	0 -4 -18	-101		
0 1 25	0 1 29	-4		
0 -4 -14	0 -3 -1	-73		
0 -4 -18	0 -3 -34	-44		

0 0 -10	0 0 -38	28		
0 -5 -23	0 -3 -58	-85		
0 7 40	0 6 27	73		
0 0 -23	0 0 -25	2		
0 2 29	0 2 30	-1		
0 -3 -30	0 -2 -51	-39		
0 -5 -16	0 -4 -51	-25		
0 2 51	0 2 51	0		
0 3 38	0 3 35	3		
0 -3 -5	0 -2 -40	-25		
0 5 52	0 5 10	42		
0 -5 -3	0 -3 -53	-70		
0 -5 -19	0 -4 -44	-35		
0 4 39	0 4 8	31		
0 2 42	0 2 53	-11		
0 0 -42	0 0 -42	0		
0 2 6	0 2 0	6		
0 0 41	0 0 38	3		
0 -2 -27	0 -2 -11	-16		
0 6 18	0 5 40	38		
0 1 26	0 1 25	61		
0 -1 -59	0 -1 -35	-24		
0 1 17	0 1 21	-4		
0 -2 -14	0 -1 -18	-56		
0 2 34	0 2 18	16		
0 0 54	0 1 9	-15		
0 0 -57	0 0 -43	-14		
0 -5 -50	0 -5 -10	-40		
0 0 -5	0 0 37	-42		
0 -1 -37	0 0 -29	-68		
0 -3 -43	0 -3 -14	-29		
0 -5 -43	0 -3 -59	-104		
0 -5 -19	0 -3 -49	-90		
0 -5 -19	0 -4 -53	-26		
0 4 40	0 4 17	23		
0 3 1	0 3 13	-12		
0 4 13	0 3 37	36		
0 0 -22	0 0 15	-37		
0 4 12	0 3 19	53		
0 3 44	0 2 55	49		
0 -5 -50	0 -4 -11	-99		
0 4 44	0 3 43	61		
0 -3 -33	0 -3 -29	-4		
0 0 -35	0 0 0	-35		
0 6 9	0 5 42	27		
0 -1 -14	0 0 -44	-30		
0 -1 -56	0 0 -55	-61		
0 -6 -51	0 -5 -32	-79		
0 0 2	0 0 -7	9		
0 -1 -45	0 0 -59	-56		
0 5 28	0 4 50	38		
0 0 -32	0 0 -13	-19		
0 -3 -41	0 -2 -30	-71		
0 -7 -32	0 -6 -11	-81		
0 -5 -37	0 -5 -11	-26		
0 3 13	0 3 1	12		
0 7 12	0 6 33	39		
0 0 -43	0 0 -35	-8		
0 2 28	0 2 32	-4		
0 0 3	0 0 12	-9		
0 -6 -50	0 -5 -41	-69		
0 1 15	0 1 21	-6		
0 -4 -49	0 -3 -23	-86		

0 -4 -46	0 -4 -9	-37		
0 -3 -15	0 -2 -5	-70		
0 -3 -57	0 -2 -39	-68		
0 4 42	0 4 4	38		
0 -5 -25	0 -3 -48	-37		
0 -1 -44	0 -1 -42	-2		
0 0 -11	0 0 -8	3		
0 6 29	0 5 48	41		
0 0 -30	0 0 -14	-16		
0 -5 -5	0 -4 -22	-43	-24.6667	-15.1667
0 -3 -16	0 -2 -1	-75	-24	-1.7500
0 0 -43	0 0 7	50	-6.6667	5.3583
0 -2 -52	0 -2 -18	-34		
0 -1 -18	0 0 -40	-38		
0 -2 -17	0 -1 -23	-54		

**THIS PAGE INTENTIONALLY LEFT BLANK**

## APPENDIX L –MATLAB CODE

```
1 %Code for the computation of platform attitude starting from Theodolite
2 %measurement. Marcello Romano/Brian Connolly, 3 May 2004.
3 - clc
4 %Theodolite measurements
5 - theodl_el = deg2rad(90,01,00);
6 - theodl_az = deg2rad(359,58,20);
7
8 - theod2_el = deg2rad(89,57,00);
9 - theod2_az = deg2rad(269,57,40);
10
11 %VOLTAGE FROM PSD
12 - ZPSD_x = -2.782384 ;
13 - ZPSD_y = -3.370383 ;
14 - XPSD_y = -0.960869 ;
15 - XPSD_x = 2.317641 ;
16
17 - ZPSD_x0 = 0.001719;
18 - ZPSD_y0 = -0.005172;
19 - XPSD_y0= 0.002559;
20 - XPSD_x0= -0.000562; %measurement
21
22
23 %
24 %THEODOLITE WORK
25 %
26
27 - D1_theod_azim_rad = 2*pi - theodl_az; %D stays for Dot on the wall
28 - D1_theod_elev_rad = pi/2 - theodl_el;
29
30 - D2_theod_azim_rad = 2*pi - theod2_az;
31 - D2_theod_elev_rad = pi/2 - theod2_el;
32
33 - r_t_theod = [-507;445;173+200] ; %mm known
34 - t_D1_theod = [6289; 0; 0]; %known
35 - t_D2_theod = [0; 16741; 0]; %known
```

```

35 - t_D2_theod = [0; 16741; 0]; %known
36 -
37 - % STEP 1
38 - delta_1_i_theod = normalize(r_t_theod+t_D1_theod); %first known vector in inertia frame
39 - delta_2_i_theod = normalize(r_t_theod+t_D2_theod); %second known vector in inertia frame
40 -
41 - % STEP 2
42 - t_D1_prime_vector_theod = azelxyz(D1_theod_azim_rad, D1_theod_elev_rad);
43 - t_D2_prime_vector_theod = azelxyz(D2_theod_azim_rad, D2_theod_elev_rad);
44 -
45 %We are here assuming that the distance t_D is not changing due to a
46 %rotation (valid for small angle)
47 - delta_1_t_theod = normalize(t_D1_prime_vector_theodnorm(t_D1_theod)+r_t_theod); %first measured vector in inertia frame
48 - delta_2_t_theod = normalize(t_D2_prime_vector_theodnorm(t_D2_theod)+r_t_theod); %second measured vector in inertia frame
49 -
50 %ASSUMING THAT T IS NOT ROTATED WR TO b
51 - delta_1_b_theod = delta_1_t_theod; %first measured vector in inertia frame
52 - delta_2_b_theod = delta_2_t_theod; %second measured vector in inertia frame
53 -
54 - % STEP 3 Algebraic attitude determination method
55 - DCM_theod = algebraic_att_det(delta_2_b_theod, delta_1_b_theod, delta_2_i_theod, delta_1_i_theod); %direction cosine
56 %matrix bi from the inertia frame to the rotated body frame
57 -
58 - Euler_angles_rad_theod = C2Euler123(DCM_theod);
59 -
60 %EULER ANGLES (123): starting from a situation with body frame aligned with inertia frame, first a rotation around xb=x1.
61 %then a rotation about yb, then a rotation about zb bring the initially frame to get aligned with the rotated body frame
62 - %rem for small angle they are all the same and the order does not matter)
63 - Euler_angles_deg_theod = [rad2deg(Euler_angles_rad_theod(1));rad2deg(Euler_angles_rad_theod(2));rad2deg(Euler_angles_rad_theod(3))]

64 -
65 -
66 %QUATERNION: TO BE DONE!!!
67 - quaternion_theod = Euler1232EP(Euler_angles_rad_theod);
68 -
69

```

```

69
70 %_____
71 %PSD WORK
72 %_____
73 - PSD1_x = XPSD_x;
74 - PSD1_y = XPSD_y;
75 - PSD2_x = ZPSD_x;
76 - PSD2_y = ZPSD_y;
77
78 - PSD1_x0 = XPSD_x0;
79 - PSD1_y0 = XPSD_y0;
80
81 - PSD2_x0 = ZPSD_x0;
82 - PSD2_y0 = ZPSD_y0;
83
84 - global AB AC CO deltax deltay
85
86 - AB = 2080;    %millimeters
87 - AC = 100;     %millimeters
88 - CO = 96;      %millimeters
89
90
91 %STEP -1 from xy measurement to azel measurement in local PSD axis
92 % %TEST
93 % PSD1_x = 5;
94 % PSD1_y = 0;
95 % PSD1_x0 = 0;
96 % PSD1_y0 = 0;
97 % PSD2_x = -5;
98 % PSD2_y = 0;
99 % PSD2_x0= 0; %measurement
100 % PSD2_y0= 0;
101 %
102
103 - PSD1_deltax= PSD1_x - PSD1_x0; %measurement

```

```

102
103 - PSD1_deltax= PSD1_x - PSD1_x0; %measurement
104 - PSD1_deltay= PSD1_y - PSD1_y0;
105 - PSD2_deltax= (PSD2_x - PSD2_x0); %measurement
106 - PSD2_deltay= (PSD2_y - PSD2_y0);
107
108 - deltax= PSD1_deltay;
109 - alpha_out = fzero(@PSD_alpha2dx,0);
110 - deltay= PSD1_deltax;
111 - beta_out = fzero(@PSD_beta2dy,0);
112
113 %STEP -0 from azel measurement in local PSD axis to azel measurement in
114 %local t axes (t is a frame located at the center of the PSD and parallel
115 %to the body frame
116 - D1_PSD1_azim_rad = pi+beta_out; %D stays for Dot on the wall
117 - D1_PSD1_elev_rad = -alpha_out;
118
119 - deltax= -PSD2_deltay;
120 - alpha_out = fzero(@PSD_alpha2dx,0);
121 - deltay= -PSD2_deltax;
122 - beta_out = fzero(@PSD_beta2dy,0);
123
124 - D2_PSD2_azim_rad = (3/2)*pi+beta_out;
125 - D2_PSD2_elev_rad = -alpha_out;
126
127 - r_t_PSD1 = [-430;0;173+140] ; %mm known
128 - r_t_PSD2 = [0;-425;173+140] ; %mm known
129
130 - t_D1 = [(r_t_PSD1(1)-AB); 0; 0]; %known
131 - t_D2 = [0; (r_t_PSD2(2)-AB); 0]; %known
132
133 %r_t_PSD1 = [-529.5;0;0] ; %mm known
134 %r_t_PSD2 = [0;-533;0] ; %mm known
135
136 %t_D1 = [(r_t_PSD1(1)-(AB-AC)); 0; 0]; %known

```

```

135 %t_D1 = [(r_t_PSD1(1)-(AB-AC)) ; 0 ; 0]; %known
136 %t_D2 = [0; (r_t_PSD2(2)-(AB-AC)); 0]; %known
138 %
139 %STEP 1
140 - delta_1_i = normalize(r_t_PSD1 + t_D1); %first known vector in inertia frame
141 - delta_2_i = normalize(r_t_PSD2 + t_D2); %second known vector in inertia frame
142 %
143 %STEP 2
144 - t_D1_prime_vensor = aze12xyz(p1_PSD1_azim_rad, D1_PSD1_elev_rad);
145 - t_D2_prime_vensor = aze12xyz(p2_PSD2_azim_rad, D2_PSD2_elev_rad);
146 %
147 %We are here assuming that the distance t_D is not changing due to a
148 %rotation (valid for small angle)
149 - delta_1_t = normalize(t_D1_prime_vensor*norm(t_D1)+r_t_PSD1); %first measured vector in inertia frame
150 - delta_2_t = normalize(t_D2_prime_vensor*norm(t_D2)+r_t_PSD2); %second measured vector in inertia frame
151 %
152 %ASSUMING THAT T IS NOT ROTATED WR TO b
153 - delta_1_b = delta_1_t; %first measured vector in inertia frame
154 - delta_2_b = delta_2_t; %second measured vector in inertia frame
155 %
156 %STEP 3 Algebraic attitude determination method
157 - DCM_PSD = algebraic_att_det(delta_1_b, delta_2_b, delta_1_i, delta_2_i);
158 - Euler_angles_rad = C2Euler123(DCM_PSD);
159 %
160 %EULER ANGLES (123): starting from a situation with body frame aligned with inertia frame, first a
161 %rotation around xb=xi then a rotation about yb, then a rotation about zb bring the initially frame to get
162 %aligned with the rotated body frame (rem for small angle they are all the same and the order does not matter)
163 - Euler_angles_deg = [rad2deg(Euler_angles_rad(1));rad2deg(Euler_angles_rad(2));rad2deg(Euler_angles_rad(3))];
164 %
165 %QUATERNION: TO BE DONE!!!
166 - quaternion = Euler1232EP(Euler_angles_rad);
167

```

**THIS PAGE INTENTIONALLY LEFT BLANK**

## LIST OF REFERENCES

- 1 B. Moore, *Flexible Multibody Dynamics and Control of the Bifocal Relay Mirror*, M.S. Thesis, Naval Postgraduate School, December, 2003.
- 2 V. Watson., *Angular Rate Estimation by Multiplicative Kalman Filtering Techniques*, M.S. Thesis, Naval Postgraduate School, December, 2003.
- 3 B.N. Agrawal, M. Romano, Ty Martinez, *Three axis attitude control simulators for the bifocal relay mirror spacecraft*, AAS 03-268, Advances in the Astronautical Sciences, Vol.115, 2003.
- 4 M.Romano, B.N.Agrawal, *Acquisition, tracking and pointing control of the Bifocal Relay Mirror Spacecraft*, Acta Astronautica, Vol.53, No.4, 2003, pp. 509-519.
- 5 M.Romano, B.N.Agrawal, *Attitude dynamics and control of a dual-body spacecraft with variable-speed control moment gyros*. Accepted for publication on the AIAA Journal of Guidance, Control, and Dynamics.
- 6 M.Romano, B.N.Agrawal, *Use of variable speed control moment gyros for a fine pointing dual-line-of-sight-spacecraft*, AAS 03-041, Advances in the Astronautical Sciences, Vol.113, 2003.
- 7 B.N. Agrawal, M. Romano, Ty Martinez, *Three axis attitude control simulators for bifocal relay mirror spacecraft*, AAS 03-268, Advances in the Astronautical Sciences, Vol.115, 2003.
- 8 R. C. Olsen, *Remote Sensing from Air and Space*. Unpublished manuscript.
- 9 Keithley, INC., *KPCI-1800HC Series PCI Bus Data Acquisition Board User's Manual*. Keithley Instruments, Inc. Second Printing 1999.
- 10 N. Pedreiro, "Spacecraft Architecture for Disturbance-Free Payload", AIAA 02-5029, 2002.
- 11 N. Pedreiro, A. Carrier, K. Lorell, D. Roth, G. Shelef, R. Clappier, and M. Gonzales, "Disturbance-Free Payload Concept Demonstration", AIAA 02-5027, 2002.
- 12 N. Pedreiro, "Spacecraft Architecture for Disturbance-Free Payload", AIAA Journal of Guidance, Control, and Dynamics, Vol. 26, No. 5, Sep-Oct 2003, pp. 794-804.

- 13 J. Stanton, "Navy, Air Force to Develop Twin-Mirror Laser-Retargeting Satellite Technology," National Defense Magazine, August 2002.
- 14 M.D. Shuster and S.D. Oh. *Three Axis Attitude Determination From Vector Observations*. Journal of Guidance, Control and Navigation, 4(1):70--77, January-February 1981.
- 15 Markley, F.L., "Attitude Determination and Parameter Estimation Using Vector Observations: Application," Journal of the Astronautical Sciences, Vol. 39, No. 3, 1991, pp. 367-381.
- 16 Werts, J.R., Spacecraft Attitude Determination and Control, Microcosm Inc., ASTROPHYSICS AND SPACE SCIENCE LIBRARY 73, December 1978.
- 17 Pittelkau, M.E., "Composite Estimate of Spacecraft Sensor Alignment Calibrations", AIAA Journal of Guidance, Control, and Dynamics, Vol. 26, No. 2, Mar-Apr 2003, pp. 371-374.

## **INITIAL DISTRIBUTION LIST**

1. Defense Technical Information Center  
Ft. Belvoir, Virginia
2. Dudley Knox Library  
Naval Postgraduate School  
Monterey, California
3. Department Chairman, Code ME  
Department of Mechanical and Astronautical Engineering  
Naval Postgraduate School  
Monterey, CA
4. Professor Brij N. Agrawal, Code ME/Ag  
Department of Mechanical and Astronautical Engineering  
Naval Postgraduate School  
Monterey, CA
5. Professor Marcello Romano, Code ME/Ro  
Department of Mechanical and Astronautical Engineering  
Naval Postgraduate School  
Monterey, CA
6. SRDC Research Library, Code ME  
Department of Mechanical and Astronautical Engineering  
Naval Postgraduate School  
Monterey, CA